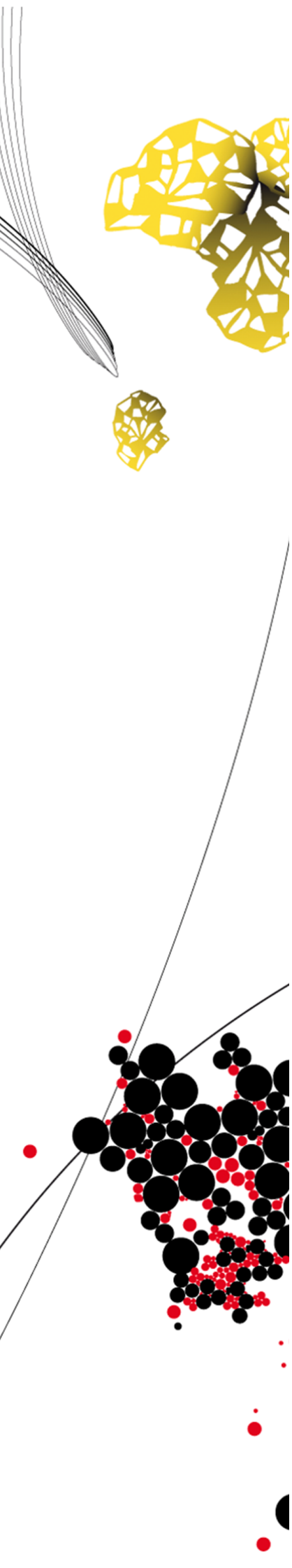

UNIVERSITY OF TWENTE.

Faculty of Engineering Technology

Deformation Analysis of Incremental Sheet Forming Process

R.A.J. Burger

Master's Thesis
January 2025

Exam committee:
prof. dr. ir. A.H. van den Boogaard
dr. ir. G.T. Havinga
dr. ir. W.B.J. Hakvoort

Nonlinear Solid Mechanics
Faculty of Engineering Technology,
University of Twente
P.O. Box 217
7500 AE Enschede
The Netherlands

This page has intentionally been left blank

Abstract

Sheet metal forming is widely used in the metal industry. These processes are usually done with dedicated tools such as a die set. While this is efficient and cheap for high-volume and low variety products, it is less suitable for production of small series, due to substantial die cost and development time. Incremental sheet forming can be used as an alternative as it does not use a die, but deforms the sheet gradually using one or more robotic manipulators. This promising production method is not commonly used yet due to limited geometric accuracy. Literature hints that using a backing force in some form can improve forming results. In this thesis, a simulation of a simplified 2D incremental sheet forming model is used to investigate the effect of the support tool on the deformation of the product. It is identified how different parameters affect the product deformation, and valuable insights are derived that can be used to properly set the position and force applied on the support tool during incremental sheet forming.

Keywords: incremental sheet forming, double-sided incremental forming, support force, local deformation

Preface

I'm writing this preface at the appropriate time and state, with cold hands due to the single glass windows in my social housing. Having finished eight-and-a-half months of research to finalize my studies, now being able to move towards the heat. It has been an interesting seven-and-a-half years, where I learned a lot, and also learned a lot in my studies. I appreciate the friends I made here and the fun I had with them that motivated me to continue my studies in the early months.

First and foremost I would like to thank Jos Havinga for his support and advice during the whole thesis. He was always interested in new findings, and gave advice using his research experience and theoreticla knowledge. I would like to thank Wouter Hakvoort for being the second supervisor. He was also enthusiastic and motivating. I would also like to thank Herman van Corbach for teaching me how to use the computational clusters at the univeristy. This saved my laptop a lot of hours. Report wise, the last one I would like to thank is my friend Hein Lucassen, for providing feedback in the early stages of writing. Finally, I would like to thank my father for always providing support, care and interest in my studies and other activities, and for being a good example in life.

Contents

List of acronyms

ISF	incremental sheet forming
SPIF	single-point incremental forming
TPIF	two-point incremental forming
DSIF	double-sided incremental forming
ADSIF	accumulative double-sided incremental forming
DoF	degrees of freedom
FEM	finite element method

Chapter 1

Introduction

Sheet metal forming is widely used around the globe, and commonly done using a die to deform the sheet into its final shape. For certain type of products, it is the preferred production method. Compared to milling, forming does not produce as much waste material, and compared to 3D printing, it is not needed to melt the material and build it up layer-by-layer. Dies can cost tens of thousands of dollars, requiring a lead time of 10 to 90 days, while being several meters in size [1]. While efficient and cheap for high-volume, low-variety products, it is expensive to manufacture low-volume, high-variety products as many dies would be needed. This results in a high die cost per produced part, requiring die development time for every new desired product, and needing to store many dies. In Figure 1.1, a sheet stamping setup that forms a car part is shown. The part is large compared to a human, and the die will be even larger. It uses a spacious metal press with a capacity of 2000 tons.

An alternative sheet forming method more suitable for low-volume, high variety production is incremental sheet forming (ISF). ISF uses a conventional CNC milling machine, or one or more robotic manipulators to shape the sheet locally and incrementally. The main advantage of incremental forming is that no die is required, saving time, money and space. Die development time is not necessary, thus new products can be produced faster. The initial setup price for new products is also reduced, as there are no costs to develop a die. This allows for pricing of parts almost independent of the volume produced, being cheaper up to hundreds of parts [3]. The process does require tool path generation for the robotic manipulators, and perhaps several iterations of product forming to get satisfying results. Space can be saved as dies that are not in use do not need to be stored anymore. Therefore, ISF can be a valuable production method for producing lower volume and higher variety parts.

The manipulator deforms the sheet with a forming tool. The sheet is fixed in place by clamps. It consists of several steps. Before the forming can take place, the desired part is designed in conventional 3D CAD software. The model is used

(a) A 2000 ton sheet metal press

(b) Car panel formed in the press

Figure 1.1: Conventional sheet metal stamping‘ [2]

for tool path generation for the robotic manipulator. During forming, the tool path is tracked by the robotic manipulator(s), and the metal sheet is deformed incrementally, layer by layer. After forming, the desired part can be cut out of the remaining sheet material. A 2D schematic drawing of the setup is shown in Figure 1.2. A real forming setup is shown in Figure 1.3, and an example of four individually formed parts can be seen in Figure 1.4.

Two more advantages are local deformation and higher forming limit. Due to the fact that ISF deforms the sheet locally around the tool tip, the forming forces are lower than conventional sheet forming. Therefore, machines with lower force capacity are now suitable to use in this metal forming process. Also the forming limit curve, the amount each material point can stretch before damage occurs, is higher, allowing the material to be deformed more before it tears. This is due to the material stress state during forming, known as the stress triaxiality. The key disadvantage is the low geometrical accuracy [3] [6], resulting in limited industrial use. The desired industry accuracy of ± 0.2 mm is not commonly achieved, as ISF accuracy is typically ± 2 mm [1].

Furthermore, as the sheet is formed incrementally, the process time is significantly higher than conventional forming. The conventional forming time per produced unit is in the order of seconds or minutes, while for ISF, 60 minutes for a single part is indicated [1]. The reduced setup time could compensate for the higher

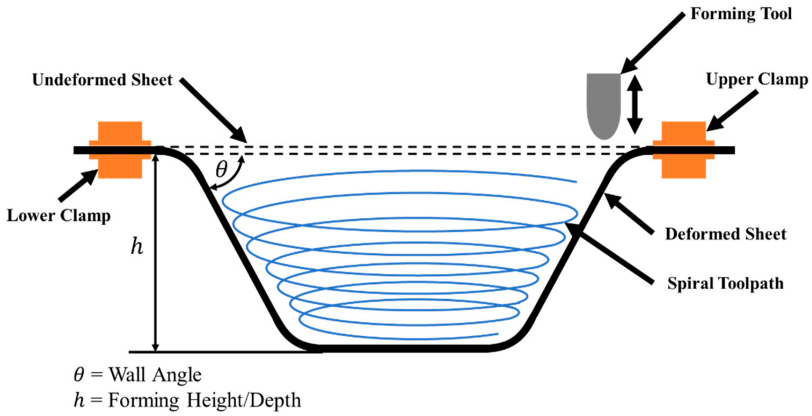

Figure 1.2: A schematic overview of the ISF process. An undeformed, straight metal sheet is clamped at all edges. The forming tool follows the tool path, represented as a blue spiral. This deforms the sheet, parameterized using forming depth h and wall angle θ. Wall angle is an important design parameter, mostly for reduced thickness reasons [4]

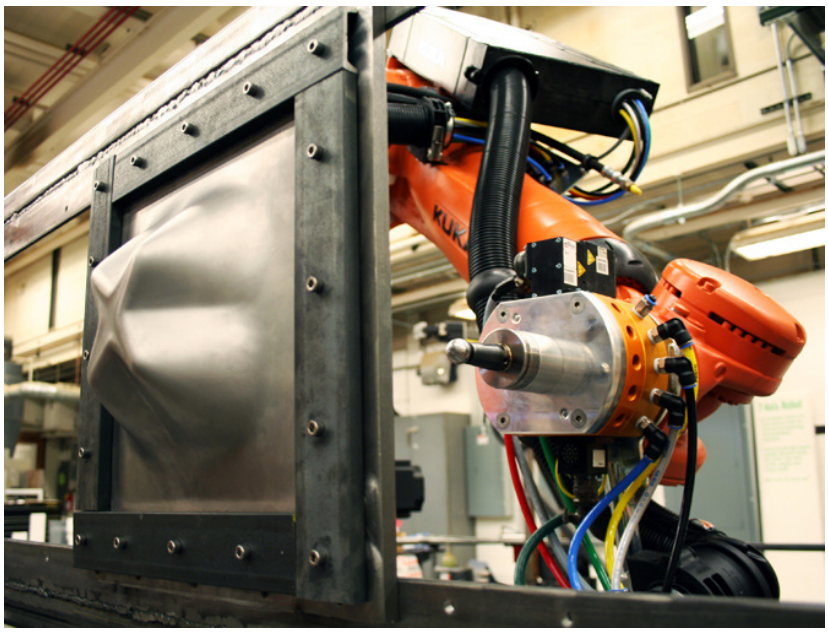

Figure 1.3: Picture of an ISF setup after forming. Setup consists of a Kuka industrial robotic arm with a forming tool, and a clamped sheet [5]. The robotic manipulator pushes the sheet from the right using a metal shank with a round tip, plastically deforming the sheet to the left. After forming, the desired part is cut out of the rest of the sheet.

Figure 1.4: Four individually formed parts using ISF. Note the forming lines on the parts, caused by incremental forming [5]

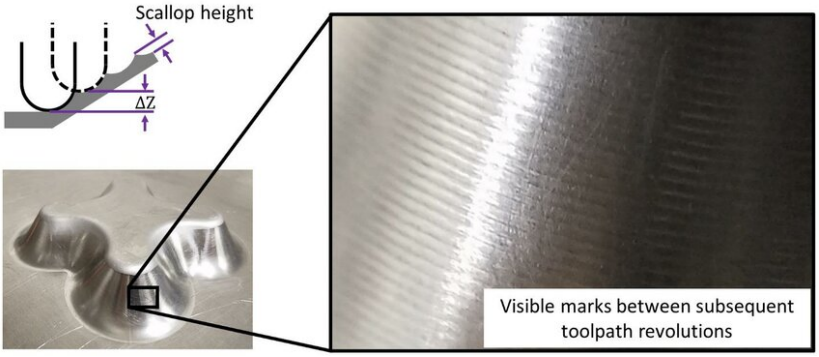

Figure 1.5: Top left shows the current tool position (solid line) and the tool position in the previous contour (dashed line). Scallops, dents in the surface, can be seen schematically and in a photo [7].

forming time for small series.

The forming time depends on the horizontal and vertical step increments between passes. Larger increments reduce the forming time, but increase the surface roughness [7]. The discrete steps create so-called forming lines, which affect the surface quality of the finished part. When taking a cross-section of a part, the forming lines are shaped like a wave on the contact surface of the part. The wave height, known as scallop height, can be related to a roughness measure. The forming lines are shown in detail in Figure 1.5.

Commercial use of ISF is limited mainly due to the lower geometrical accuracy. Two commercial examples are Amino North America Corporation and Machina Labs. Amino North America Corporation [8] has used ISF since 2002, with many

applications, one of which is producing the hood of a Honda S800 [9] . Another company in North America, based in Los Angeles under the name Machina Labs has been active in the ISF industry since 2019. Amino uses ISF with a partial die; it is a smaller, simpler die that can be used for multiple shapes. Machina Labs on the other hand uses a second robotic manipulator to provide a backing force.

Applications in research are for example in the biomedical sector such as foot orthosis and skull implants [3], or for prototyping parts that will later be formed in more conventional ways. In architecture it can be used to form double curved panels. Ironically, ISF can be used to make dies. Not for sheet forming, but as a mold for composites, being quicker, cheaper and lighter than conventional milled molds [10].

One can see that ISF has great potential, but it is not yet common practice, mainly due to the lower geometrical accuracy. The lower geometrical accuracy is largely caused by the limited locality of the applied deformation. When comparing single-point incremental forming (SPIF) with two-point incremental forming (TPIF) or double-sided incremental forming (DSIF), it is clear that the latter two solve some of the issues of single point due to both providing a support force on the other side of the sheet. The backing force can be used to localize deformation and to increase its plastic deformation. Comparing both options that provide a backing force, DSIF is more flexible as no (partial) die is needed. However, limited literature is available about how to localize plastic deformation in ISF in general, and for DSIF, it is not clear how that can be done using the support tool. As DSIF is more flexible, in this research, the focus is upon determining how the support force in DSIF can be used to localize deformation and by doing so improve the geometric accuracy of the process.

The report is outlined as follows. In Chapter 2, a literature review is performed for solutions to the described problems in ISF. The literature gap and research goals will be explained in more detail. The methodology used to investigate the research questions will be described in Chapter 3, and the results will be discussed in Chapter 4. Disussions, conclusions and recommendations are in Chapter 5.

Chapter 2

Literature review

As discussed in the introduction, ISF can be economical for low-volume high-variety products, but its use is limited mainly by the geometrical accuracy. This chapter will study literature on that topic in more detail. In this research, it will be investigated how the accuracy of ISF can be improved by using a support tool.

First, the forming process is described in detail. Then, a literature review is performed to find out what methods are available to improve geometrical accuracy. Special attention is given to tool path generation, forming simulations, and process control. The gaps in literature will be identified and used as a starting point for this research.

2.1 The incremental forming process

The principles behind ISF was explained briefly in the introduction. An overview of the steps is shown in Figure 2.1. The forming process is explained in detail in the following sections.

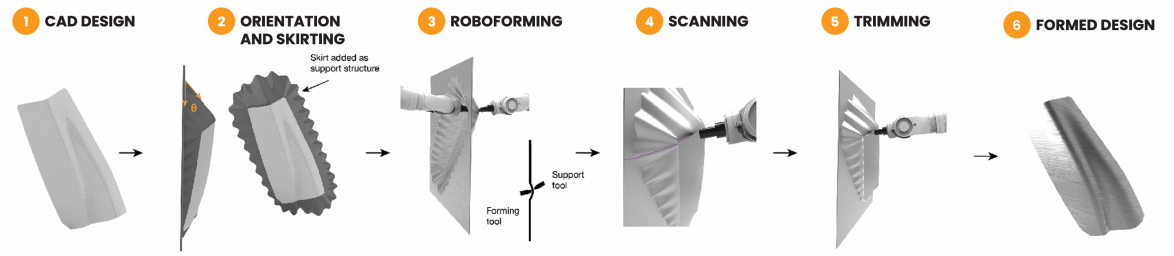

Figure 2.1: Overview of whole forming process, adapted from [11]. Skirting is added to the CAD design, such that the wall angles are more favorable. After forming, the part can be scanned for quality check, or for adjusting the part. Then, the desired part is trimmed from the rest of the sheet.

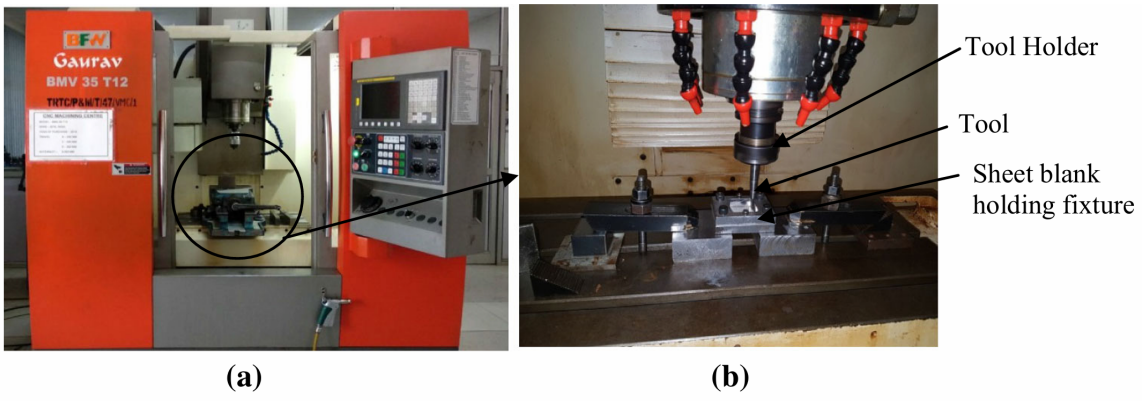

Figure 2.2: SPIF setup using a conventional 3 DoF CNC milling machine: BFW model BMV 35 T12 [13]

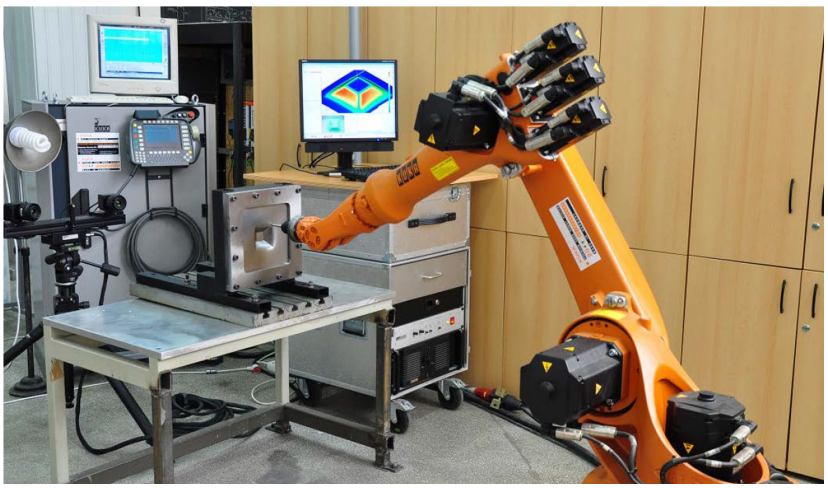

Figure 2.3: SPIF setup using a KUKA KR6-2 robotic manipulator [14]

2.1.1 Incremental sheet forming setup

The robotic manipulator pushes typically with a force of a few hundred Newtons [12], which could significantly flex the forming setup. Therefore, a stiff setup is desired, and conventional 3 degrees of freedom (DoF) CNC milling machines are a suitable choice, such as in Figure 2.2 by [13], which uses an BFW model BMV 35 T12. The sheet metal blank is kept in place by the blank holding fixture. The machine moves the tool onto the sheet.

Industrial robotic manipulators also have found their use in ISF. Although lower in stiffness, they offer more DoFs thus more design freedom. Crenganis [14] uses a KUKA KR6-2 industrial robotic manipulator, shown in Figure 2.3.

ISF so far has been said to be dieless. Variants of ISF exist where a (partial) die is used as a support for the back side of the sheet. This can be a full die, i.e. the exact shape of the part to be formed. Or partial dies, such as a simple cylinder,

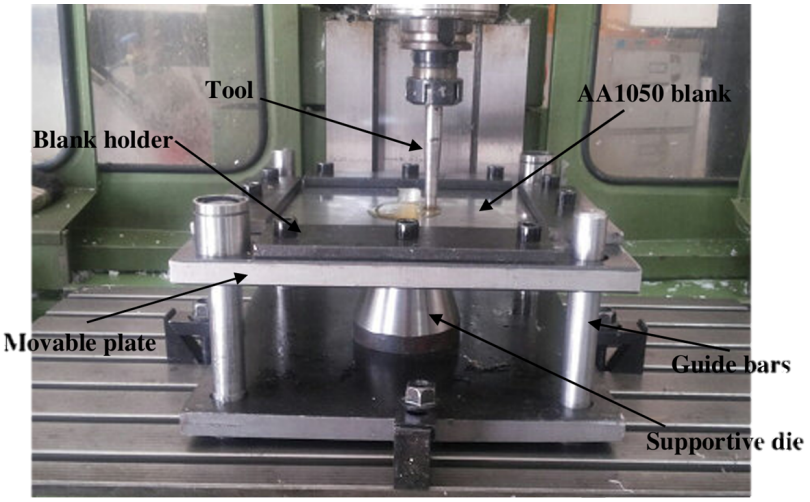

Figure 2.4: Incremental forming setup with a partial die, which can be used to form several different parts. Adapted from [15]

which can be used for several different parts. An example of a partial die is shown in Figure 2.4. The blank holder holds the aluminum blank. For every contour, the movable plate moves the sheet onto the supportive die and then the tool forms the sheet around the partial die.

Instead of using a partial die, a second forming tool can be used for support. This allows for the most flexible setup, as not even a partial die is needed. Two examples are a CNC style setup and a robotic setup. Custom CNC milling style manipulators such as Figure 2.5 are parallel manipulators in a stiff configuration. One tool is used to deform the sheet, and the other tool to support the sheet. Robotic manipulators are demonstrated in Figure 2.6.

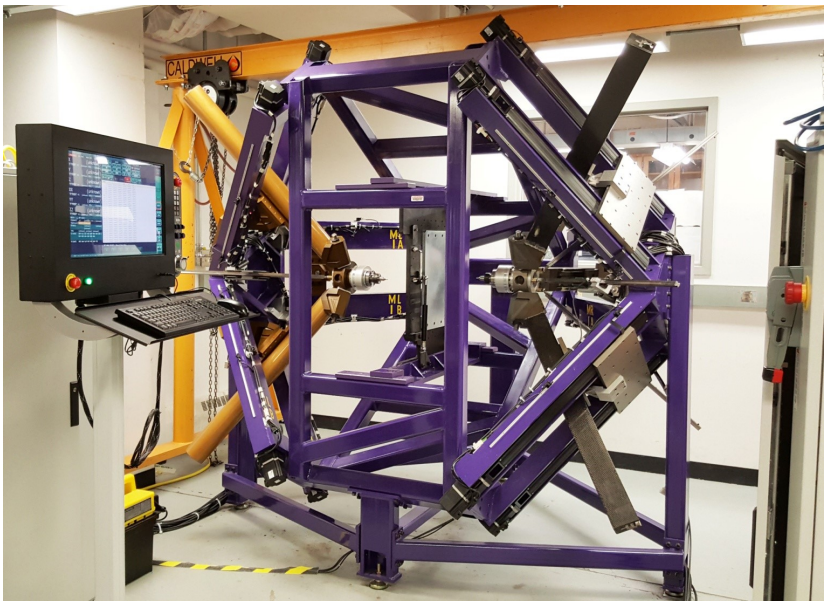

Figure 2.5: An DSIF incremental forming setup using two parallel manipulators in a stiff configuration [16]

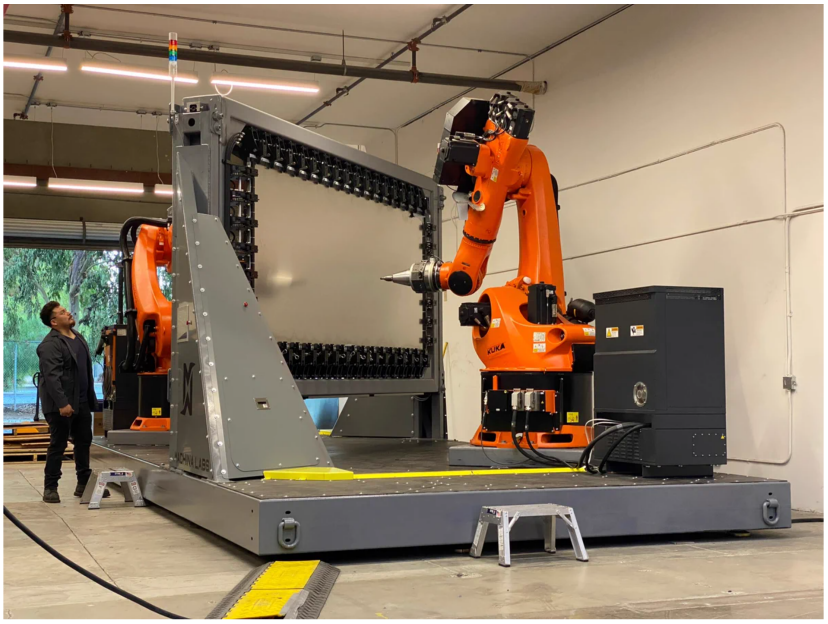

Figure 2.6: An DSIF setup in a commercial application [17]

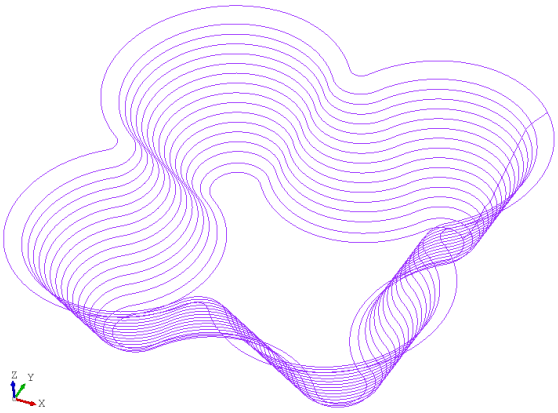

Figure 2.7: A tool path example, built out of consequent closed contours [7]

2.1.2 3D CAD design and tool path planning

The part to be formed can be designed in conventional 3D CAD software. The orientation of the part onto the sheet can be chosen such that the formed wall angles are more favorable. Optionally, skirting can be added, as seen in step 2 of Figure 2.1. Skirting increases the stiffness of the first few layers of ISF [10]. This makes the sheet more stable for the remaining contours.

A tool path can be generated purely on the geometric properties of the part, similar to conventional CNC milling. This does not take material springback into account, which can result in significant deviations. The tool path can be a continuous path, from the initial depth to the final depth, often representing a spiral. It is also possible for the tool path to be cut into discrete closed contours: one closed contour for every depth increment. An example can be seen in Figure 2.7.

Tool paths can be improved by taking into account process properties such as springback. This can be done in simulations before the process starts, or tool paths can be updated iteratively when forming the same part multiple times. For DSIF, path planning needs to be done for both tools. One of the tools is seen as a support tool, and is positioned relative to the forming tool based on a position [7] and/or force requirement [10]. Tool path generation will be treated in detail in the next chapter.

During the forming process, the tools interact with the sheet to deform it. finite element method (FEM) simulations can be done beforehand in order to check product properties, such as excessive thinning, occurring of damage and springback. However, simulating this in detail can become too expensive. Simple rules to estimate for example wall thickness exist, such as the sine rule [18], where the wall thickness has a trigonometric relation with wall angle. The method is limited in accuracy, as it assumes constant wall thickness across the formed part.

2.1.3 Forming mechanics

The forming mechanics will be explained for several ISF setups, as different effects cause different deformations.
SPIF is the simplest setup with one forming tool and a clamped sheet, as was seen in Figures 1.2 and 1.3. The manipulator pushes the tool into the sheet and moves it around. The tool exerts a force onto the sheet, causing the sheet to deflect as it is only supported at the edges. This causes elastic strains. If the force is increased sufficiently, plastic strains will occur. When removing the tool contact and when releasing the product from the clamps, the product finds a new equilibrium state, in which a large portion of the elastic strains vanish. This causes deformation of the product, called springback.

In SPIF, the tool touches the sheet on one side and applies a force. This causes the whole sheet to deflect. If the sheet would be supported on the other side, deflection can be reduced, decreasing the amount of elastic deformation. It might be useful to apply a counter force to the sheet, to reduce the global elastic deflection, and to increase the local stress concentration. A counter force can be achieved by using a partial die such as in TPIF, shown in Figure 2.4. The partial die prevents the sheet from deflecting globally. The applied force is now more local, causing increased local plastic deformation and reduced global elastic deformation as was desired.

As mentioned in Section 2.1.1, a second forming tool can be used as a support instead of a (partial) die. This gives more freedom for the support positioning, allowing more complex shapes.

For DSIF, no clear guidelines are available on how to use the support tool to localize the deformation, or more specifically localize the plastic deformation.

2.1.4 Monitoring and control of the forming process

During forming, the process can be monitored by using sensors, and adjusted by deviating from the tool path, in order to improve several aspects of the process. One could make use of 3D scans of the partial formed product to adjust future contours [19], or measure the applied force of the manipulator to for example, to either make sure that a constant force is applied [20] or to predict springback [21]. This topic is treated in detail in Section 2.3, where offline and on-line control systems in ISF are mentioned.

2.1.5 After forming

After the forming is done and the tools are retracted, the part can be trimmed out of the formed sheet. The trimming can be done using the same robotic manipulator by (autonomously) switching its end effector [10]. The skirt support structure is separated from the desired part. Some additional springback due to part release is experienced. The part can now be treated further until ready for use.

2.2 Tool path planning

The tool path tracked by the robotic manipulator(s) determines what part is formed. Generating those paths can be done purely on geometrical properties, or by also including mechanical considerations such as material behavior. A software program to develop tool paths using geometrical properties is shown in Section 2.2.1. Also other methods including mechanical behavior, mostly springback, will be highlighted.

2.2.1 Geometrical tool path generation example

Tool paths can be generated most easily by following the contours of the desired part. For SPIF, this is trivial. But for TPIF and especially DSIF, it is harder. A PhD student from Northwestern University [7] has developed tool path software for incremental forming [22]. It is suitable for all three variations mentioned in this paragraph, and also accumulative double-sided incremental forming (ADSIF), which is similar to DSIF, but now with the spiral shaped tool path going from deep to shallow which is inside to outside. The tool path is determined based on geometry alone, accounting for sheet thickness, tool radius and shape, contour step heights, and more. The depth increment can be automatically adjusted based on varying wall angle, shown in Figure 2.8. This makes the resulting scalloping height more constant along the part, improving the surface finish. For DSIF, the software can include a squeezing component: how much to squeeze the sheet in thickness direction between the two tool contact points. More about squeezing in tool paths is explained next.

2.2.2 Geometrical tool path planning for DSIF

The effect of squeezing factor on forming results is studied in [23]. The tool path of the support tool is determined based on the path of the forming tool. The sheet thickness is estimated using the sine law, and this estimation is then modified by the squeeze factor such that the support tool compresses the sheet to a certain extend. The factors of 1.0 (no squeezing), 0.9 and 0.85 were used in the paper. 0.9

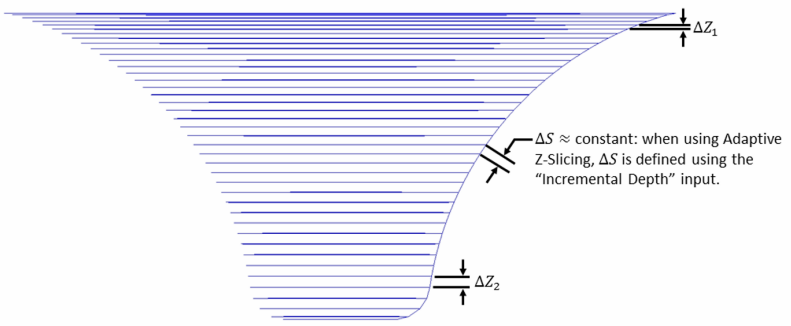

Figure 2.8: From [22]

improves the forming results over 1.0, but 0.85 showed tool marks due to increased compression. The support reduces deflections outside of the forming region. If support tool contact is lost, deflection occurs mostly between the formed region and the clamps, as the formed region has a higher stiffness due to its shape and work hardening. The main drawback of this approach, is that support tool contact is lost when unexpected thinning occurs. The researchers mention force control as a possible solution for maintaining contact.

2.2.3 Improving tool paths by using mechanical properties

Tool paths can be further improved by taking into account mechanical properties of the forming process. This can be done using experiments or simulations. For simulations, FEM is often used. Simulations can be done like conventional forming using a die, or by simulating the full ISF process using a tool to deform the sheet incrementally. Springback estimation can be used to improve the initial tool path before forming.

Certain requirements may be set for the local wall thickness at certain positions in the product, which may require adjustment of the tool path in order to satisfy these requirements. In general, the larger the wall angle, the more thinning occurs, as demonstrated in Figure 2.9. In the figure, one can also see how skirts can be generated to reduce the wall angle for forming. Excess material is trimmed away after forming. Adjusting the forming strategy may be required to achieve wall thickness requirements. One example is multi-stage forming. With multi-stage forming, the final wall angle is formed in multiple stages, each stage increasing the previously formed angle. This can reduce sheet thinning [24]. Based on simulations and experiments, it is found that wall thinning decreases with decrease in initial wall angle, and increases relatively to the thickness of the sheet. A schematic drawing of multi-stage forming is shown in Figure 2.10. An example of a part formed using multi-stage forming is shown in Figure 2.11. A square cup is formed in four stages.

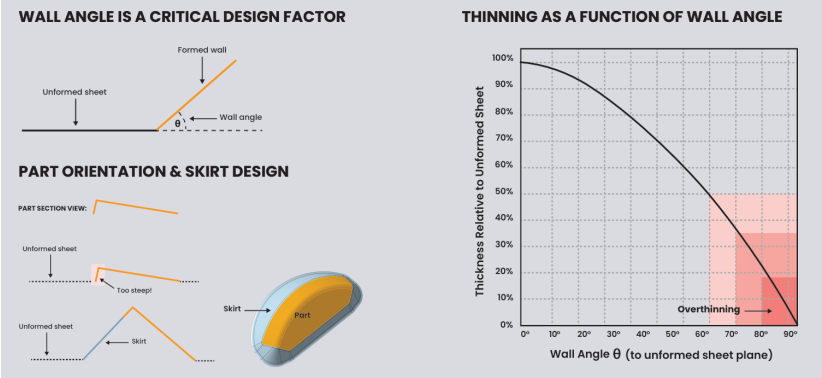

Figure 2.9: Wall angle in incremental forming. The angle can be reduced using skirts. Wall thinning depends on a function of wall angle. From [11]

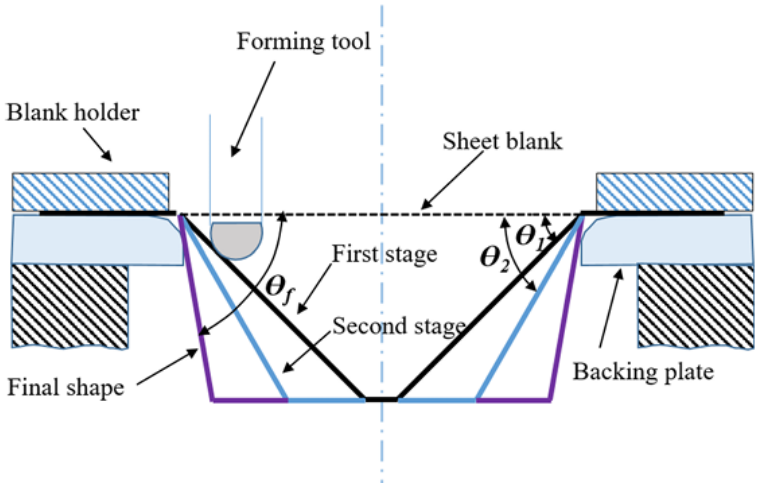

Figure 2.10: Schematic overview of multi-stage forming. The part is formed in several stages, starting with a low wall angle that is increased each stage [24].

The wall angles are formed at 45° and in the next stage extended to 90°. Without multi-stage, the 90° wall angle would not be possible, as thinning would become too much. Multi-stage distributes the material differently, allowing for higher wall angles.

2.3 Control for improving incremental forming accuracy

While incremental sheet forming has been researched since 1989, the forming process was using open loop control up until 2012 [19]. Open loop control means that the complete tool path is determined beforehand. No measurements are taken dur-

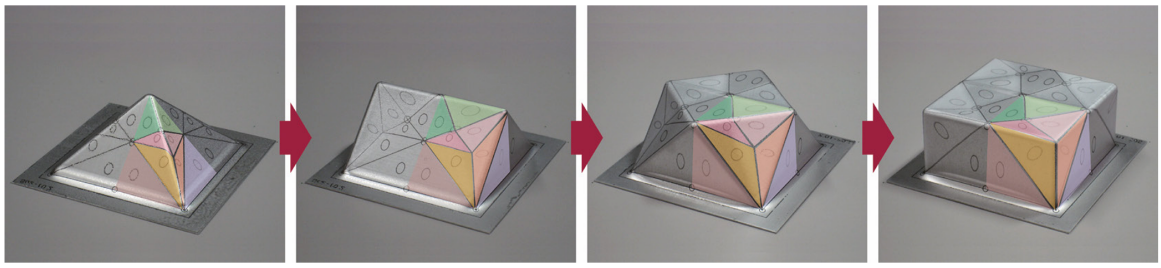

Figure 2.11: A square being formed in multiple stages, achieving a total wall angle of 90° [25].

ing forming, and no corrections to the tool path are applied during forming. Therefore, the accuracy of forming drops if unmodelled phenomena come into play, such as material property deviations. Closed loop control can compensate for forming deviations by using measurements and adjusting the forming process accordingly. It can be applied during forming, which is called on-line closed loop control, or in-between forming the same part multiple times, which can be seen as offline closed loop control. Up until 2009, on-line control for ISF has not been achieved due to insufficiently fast modeling techniques. Modeling of ISF is slow due to its non-linear deformations and its history dependence (future deformations depend on previous deformations). Several control methods that are able to improve geometrical accuracy will be treated in detail, to get an idea of investigated options.

2.3.1 Offline control

One of the more rudimentary approaches to control incremental forming could be to form the part in full and check where geometrical deviations occur compared to the desired part. Based on the geometrical deviations, the tool path can be adjusted when a second part is produced. This can be done iteratively, such as in [26], where the surface of the fully formed part after springback is measured with a 3D scanner. The surface of the formed part and desired part are linked together using the Fourier and wavelet transforms. Using this deviation, the tool path is adjusted to next time form a part closer to the desired shape.

The previously mentioned control method requires forming a part multiple times to improve the forming accuracy. It is also possible to estimate the final shape using simulations. In simulations, forming tools can follow along the calculated tool path and deform the sheet incrementally. Then, the tools can be retracted and the sheet can be released from the clamps in the simulation. Without actually forming, the simulation gives an estimate of forming results. The advantage of actually forming is that it will be more representative for the actual part than simulations. It can also be

faster than simulating the process [10]. Not considering time savings, forming will be more expensive than simulating, as the forming setup will be occupied and could not be used for e.g. commercial purposes, and also sheet material is consumed.

Instead of creating a new part every time, it is also possible to improve an individual part after forming. After forming, the part is measured using a 3D scanner. Regions with e.g. high geometrical deviation are detected and compared to the desired shape. This is translated to tool paths to touch upon the part, comparable to how a human craftsman would form a piece iteratively to the final desired shape. It is for example mentioned in [10]. It is different from multi-stage forming, as multi-stage forming has the goal to form the final wall angle in multiple steps. Multi-pass tries to improve a formed part by touching up on deviations. Multi-pass might be combined with multi-stage, for example touching up at an intermediate or final stage of the forming process.

2.3.2 On-line control using impulse responses

The first on-line, closed loop feedback system in ISF models the control actions using impulse responses, which is a common time domain control method [27]. During forming, the manipulator tracks the predetermined tool path. After every forming pass, meaning after every tracking every closed, discrete contour, the tool is retracted and some springback occurs. Then, a 3D scanner measures the shape of the (partially) formed sheet, and deviations to the target shape are used to trigger control action impulses. One such impulse is shown in Figure 2.12. With impulse, the authors mean an indentation of the forming tool into the sheet. Creating such an impulse causes the sheet to deform mainly close to the tool, although some deformation occurs in regions further away, indicating limited locality. Considering an axi-symmetric part, such as in the paper, one impulse per contour is required to understand the effect of the impulse on the final target shape. Considering N contour lines, this requires 2N experiments or simulations, for every part. For non-axisymmetric parts, multiple impulses per contour are required. Thus, impulses can become costly information to achieve. Other drawbacks is that effects between consequent impulses are not taken into account, limiting accuracy.

One possible improvement is to estimate how future impulses will behave based on previous impulses and their influence on the current shape. This is done in [28], where a learning module is added to the MPC controller to estimate future impulses. It can estimate all future impulses and optimize their contributions to the final shape before each forming pass. While improving results, it still suffers from the main limitation of impulses, namely their unaccounted interaction.

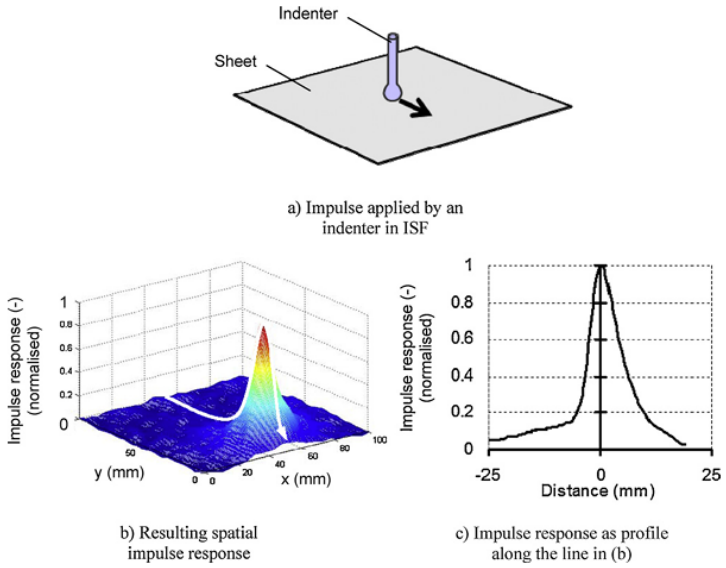

Figure 2.12: Modeling method using so called impulse responses. The tool is indented into the sheet, retracted, and the deformed surface is measured by a 3D scanner. Deformation occurs over an area wider than the tool tip, suggesting deformation is limited in locality. From [19]

2.3.3 On-line control for springback compensation

A third control method is based on springback estimation, as it can be considered one of the main causes of geometric deviation [12] [21]. The process is performed using the nominal tool path, generated by some algorithm. The nominal tool path is the initial tool path the manipulator will track. Control actions will cause deviations of the nominal tool path in order to improve the final product geometry. At certain intervals along this tool path, offline estimations are made for the relationship between tool force (tool-sheet contact force) and deflection of the partly formed sheet. Measuring the forming force during the forming process can thus give an indication of expected springback, and the expected springback can be used to improve forming by deviating slightly from the nominal tool path.

This is demonstrated in Figure 2.13. Using the original tool depth, seen as the yellow line in the left figure, will result in a lower than desired depth, represented as the blue line in the left figure. This is due to springback, indicated with z_Δ in the figure. Modifying the tool path based on expected springback is done in the right figure. After springback, the depth is as desired, and thus is the springback compensated.

The expected springback and forming force relationship can be found in multiple ways. Two will be highlighted: a numerical approach using FEM, and an analytical

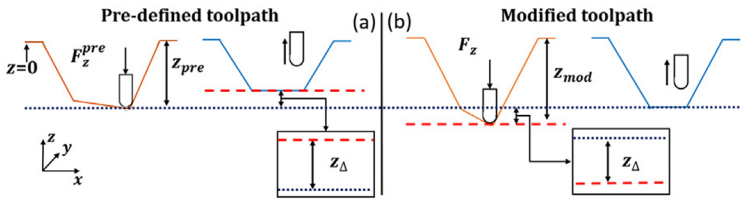

Figure 2.13: Compensation of tool path depth to take into account springback. The expected springback z_Δ is used to increase the tool path depth, such that the desired depth is achieved after springback. From [12]

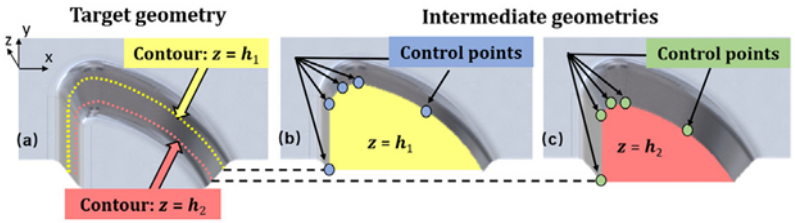

Figure 2.14: In the figure, two consequent contours are shown which can be fully represented by a limited amount of points: control points [12]

method using beam models.

Numerical springback estimation

Ren [12] uses FEM to estimate displacement for a given force measurement, and adjusts its tool path for future contours based on that. The tool path key features are captured at specific points along the path, called control points. The goal of using control points is to estimate the behavior of the whole contour, based on the behavior of a few points along that contour. An illustration of control points used is shown in Figure 2.14. For every contour, here h_1 and h_2, a limited amount of control points are selected at critical locations.

The sheet is loaded during forming, and will deflect according to its stiffness. This stiffness can be used to estimate springback after the forming tools release contact. Using simulations, the stiffness is calculated at control points over a force range. Doing these simulations for all path points would be unfeasible due to the computational cost thereof.

The displacement is equal to the springback. The result of one simulation is shown in Figure 2.15. The displacement is simulated for a range of forces. A power function represented by two parameters is fitted to the outcome of the simulations. This function can be used to estimate springback during forming, as it is now a quick calculation compared to FEM.

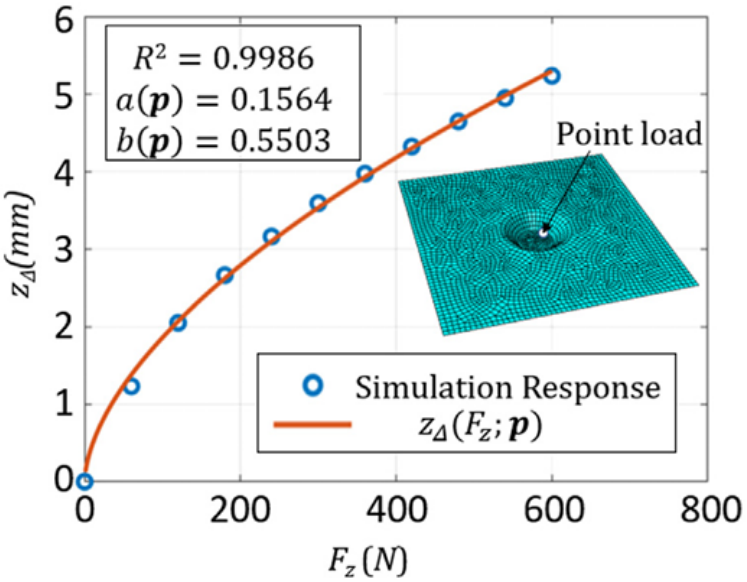

Figure 2.15: Control point deflection is simulated for a range of tool forces at a specific forming step. The results are fitted with a power function consisting of two location-dependent parameters a and b [12]

For a truncated cone such as the sheet in Figure 2.15, the average error of 3.1 mm was improved with this control method to 0.8 mm, on a total depth of 20 mm. The peak error was reduced from 5.7 mm to 1.5 mm. In the bottom area of the produced part, the method is less effective, as the error in that section is caused by someting called the pillow effect. This effect is the bending of the bottom part due to compressive stresses on the edges of the section. These compressive stresses are caused by the springback force of the sidewalls, which tries to compress the bottom section in its longitudinal direction.

The advantage of this approach is that it is able to reduce springback error in the first forming attempt for non-trivial geometries. Little equipment is needed, a just a force sensor is used.

Analytical springback estimation

The springback can also be estimated using an analytical approach instead of a numerical simulation.

One such example is by dividing the part into three regions, namely two bend zones and one inclined wall zone. Each zone can cause springback, and is therefore included in the analytical model. The bend is modeled as a curved beam, and the inclined wall as a straight beam [21], shown in Figure 2.16. A force sensor is required for this method, as the force is used in the analytical model in combination with the

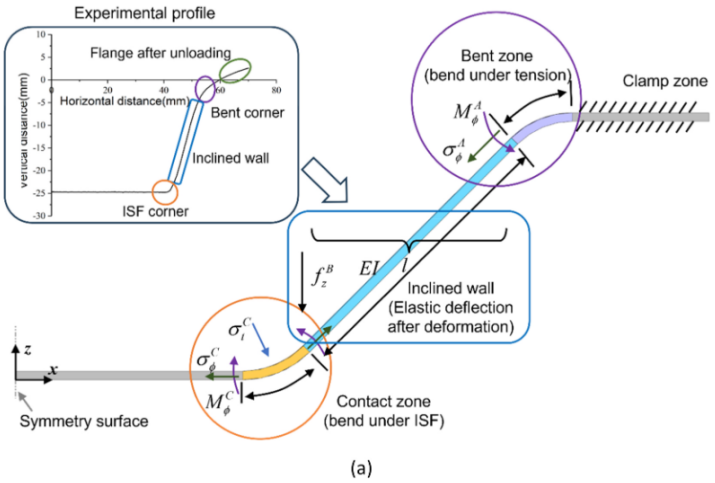

Figure 2.16: Representation of sheet during forming. Springback is estimated by modeling the sheet as two curved beams (bend zones) and a straight beam (inclined wall). From [21]

stiffness of the beams to estimate the deflection of each beam. The deflection ratio between the beams is then used to predict the springback, and that value is finally used to compensate the tool path to improve accuracy.

2.3.4 On-line control of support tool force

A crucial aspect of DSIF is the constant contact of the support tool. If contact is lost, tearing can occur [20]. A commercial user mentions that a certain support force target needs to be reached, in order to stabilize the deformation [10]. Stress triaxiality paper states that deformations can be larger due to the support force causing a certain stress triaxiality .

If the manipulator is force controlled, reaching a target force is trivial. If the manipulator is position controlled, as is common in industrial manipulators, a position-force relation needs to be established. A method to achieve this will be explained. A target force needs to be reached by the support tool. The currently applied force is measured using a force sensor between the tool and the manipulator. This value is compared to the target force, and the force error is calculated. As the manipulator is position-controlled, the force error is translated into a positional error using Hooke's law and three model elements with limited stiffness. These elements, shown in Figure 2.17, take into account the stiffness of the robotic manipulator, the stiffness of the forming tool attached to the manipulator, and the sheet stiffness felt when squeezing the sheet in thickness direction. Using these stiffnesses combined in series gives us a single position-force relation. The force error can be translated into a position error, and this can be used in the already implemented positional control loop of

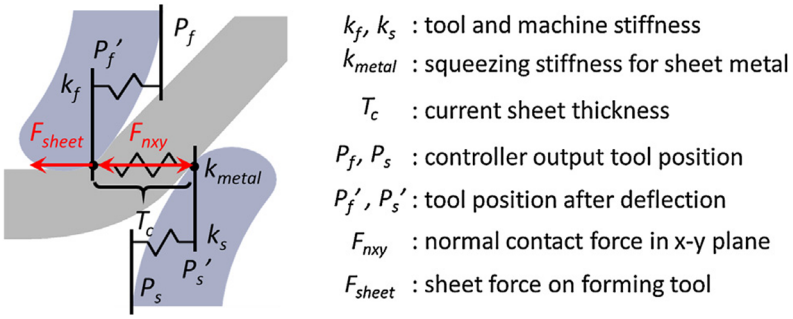

Figure 2.17: Modeling of two forming tools with bending compliance and the compressible sheet as springs, to achieve a relation between squeezing force F_{nxy} and robotic end effector positions. From [20]

the manipulator. The support tool can now be force controlled, which keeps contact with the sheet, independent of sheet thickness, improving forming characteristics. Achieving a target force can also be used for manipulator compliance compensation [10].

2.4 Research gap

To summarize this chapter, many methods exist to reduce the main problem with ISF, namely its geometrical accuracy, all to a varying degree but with limited success. The control methods suffer from the difficult-to-predict deformations, and the methods used in literature had their limitations. In general, the control methods all influence the global shape by elastic deformation, instead of focusing on introducing local behavior. Literature hints that providing a backing force on the other side of the sheet can increase locality and increase plastic deformation. Also, the backing force could reduce the clamping forces, concentrating the stress field more towards the forming area. However, no clear guidelines are available for DSIF, about the tool positioning or tool force. Therefore, the goal of this research will be to find out how to use the support tool to provide a backing force, with the goal of reducing springback and plastically deforming the sheet around the tools.

Chapter 3

Methodology

To find out how to use the support tool, one could use experiments, analytical approaches and simulations. Analytical approaches were not found in literature, as the process is expected to be too complex. In this work, the required support tool force and other parameters will be investigated by numerical simulations. A parameter grid search will be conducted to find out what inputs can produce satisfactory outputs. Simulations can be used to get an initial estimate, and are easy to automate for a search. The simulation model will be explained first, along with its inputs and outputs. Then, the three chosen parameter studies are motivated.

3.1 Simulation model setup

The simulation is done in Abaqus, which is a FEM program suitable for non-linear simulations.

3.1.1 Simulating in 2D

The problem will be reduced to 2D, as that is cheaper to simulate and the expectation is that less physical phenomena come into play. This might make it easier to understand the mechanics happening during forming. In case of 3D ISF, major deformations happen along two axis, thus simplifying to plane strain in 2D could be seen as reasonable. Plane strain is therefore used in the simulations.

In 2D, the sheet could be seen as a strip of metal with infinite width. The tools form along the whole width, thus can be seen as cylinders with infinite length. This is different from the 3D case, where tool tips can have e.g. a spherical shape.

In 3D ISF, the two tools touch the sheet at one point each, near each other. To form a product, these tools move all over the sheet, and slowly increasing depth from outside to inside or the other way around. The sheet is not loaded symmetrically.

In the 2D case, this would correspond to a forming increment on one side of the sheet, followed by a forming increment on the other side of the sheet. This will also load the sheet non-symmetric. It is assumed that loading the sheet non-symmetric increases the complexity of the mechanics. To prevent that, a symmetric loading will be used. This can be done using two tool pairs, or with a symmetry in the middle of the sheet. If forming with symmetry is successful, the symmetry can be removed, and the sheet can be formed one side at a time to slowly increase model complexity towards the real forming process. This verification can also be done in 2D allowing for cheap simulations, but does not verify the case for 3D.

In the model, the sheet is clamped on the left side, thus the edge of the sheet is fixed. On the right edge, there is a symmetry boundary in x-direction, thus fixing those nodes in horizontal direction and not allowing rotation of the right edge. This gives the same result as using four forming tools.

Comparing the 3D sheet with the 2D strip, one could reason that the strip is less stiff than a sheet. If pushed by only one tool, a strip will deflect more and less local than the sheet. Therefore, forming is expected to be less successful without some form of backing force. Adding a backing force, provided by the support tool, makes forming in 2D plausible. The 2D simulations can be thought of as incremental strip forming, rather than incremental sheet forming.

3.1.2 Parts

The sheet is modeled as planar solid elements, with deformable discrete elements. The full sheet is 200 mm long and 1 mm thick. Because of symmetry, the sheet is 100 mm long in the model, representing a 200 mm long sheet. The tools are modeled as rigid, analytical partial circles.

3.1.3 Material modeling

The material is an relatively easy to form aluminum. It is modeled as elastic-plastic behavior. Elastic behavior uses a Young's modulus of 70×10^3 MPa and a Poisson's ratio of 0.3. The plastic behavior uses Johnson-Cook hardening law, with hardening parameters $A = 300$, $B = 200$, and $n = 0.4$ without temperature effects. Using these parameters, the relation between yield stress and plastic equivalent strain is shown in Figure 3.1.

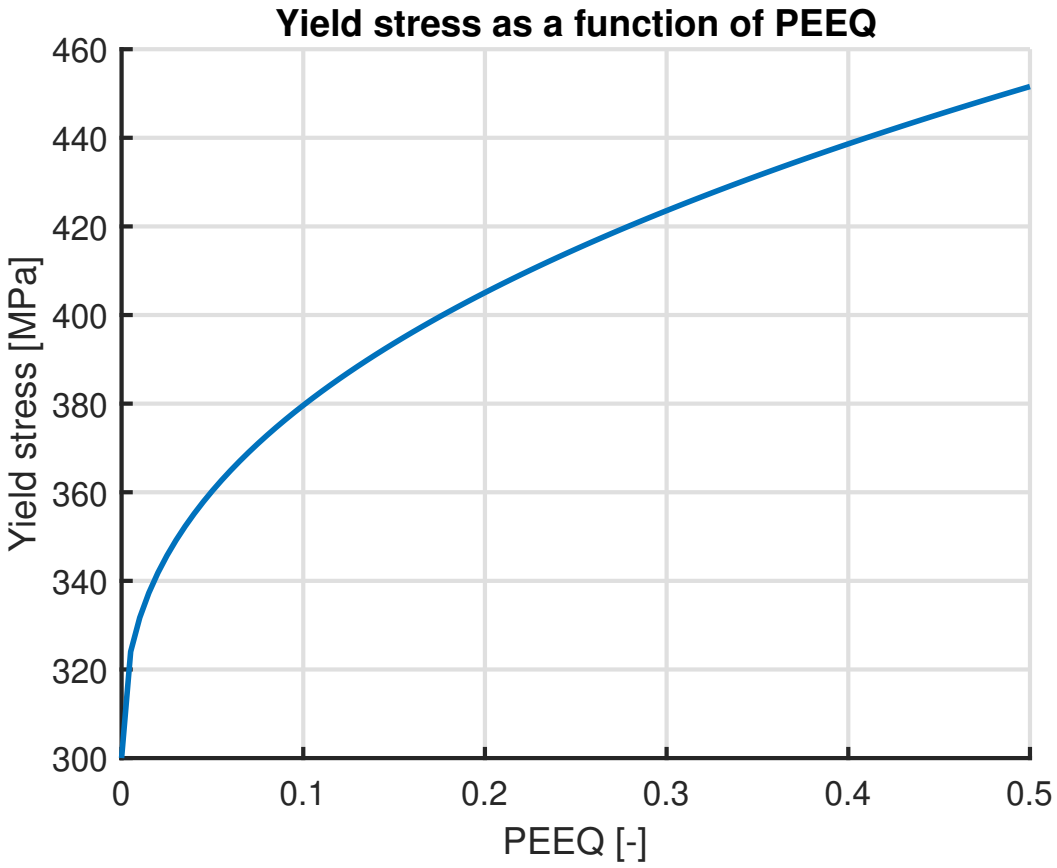

Figure 3.1: Material hardening curve, with the yield stress as a function of plastic strain

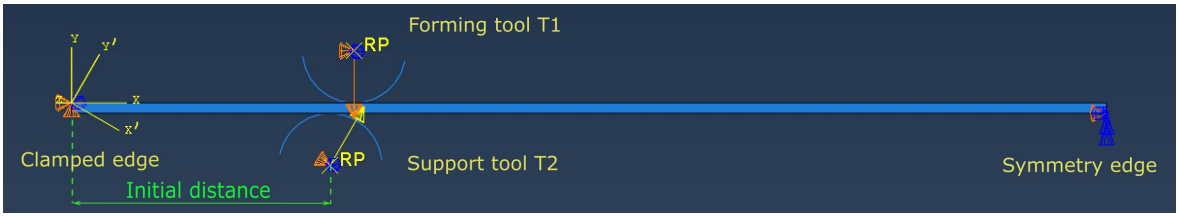

Figure 3.2: Overview of simulation boundary conditions and loads.

3.1.4 Steps, boundary conditions, and loads

The tools could be controlled in position, force or a combination of the two. The goal for the forming tool is to push into the sheet along the predetermined tool path which should successfully form the desired part. The support tool will have to push the sheet back to localize the applied stress. This could be done using position control. However, as stated in the literature, the drawback of support tool position control is that the thickness of the sheet needs to be known exactly during the whole process. This is unfeasible, as expensive simulations would be required. Therefore, the support tool will be force controlled along one direction, always assuring contact. The tool is fixed in position in the other direction, and this position is determined relatively to the forming tool.

The simulation consists of three steps: the forming step, the tool release step, and the clamp release step. During forming, the tools move into the sheet. Then, the tools are retreated (contact is disabled) in the tool release step. After the tool contacts are released, the sheet clamps are released as well by turning off these boundary conditions. The left bottom node is fixed in position and orientation, such that springback occurs properly and the part does not experience rigid body modes.

The forming tool, tool 1, is position controlled in most of the simulations, and is pushed into the sheet. The support tool, tool 2, is constrained in one direction and its rotation, and force controlled using a load in the other direction towards the other tool, in an attempt to localize the deformation during forming. An advantage of force control is that it will remain in contact even when unexpected thinning occurs. In the other two simulation steps, it is fixed in all directions. The position controlled tool 1 moves into the sheet with depth PD. The force load $T2_F$ is used during forming. The sheet is clamped on the left, and has a symmetry boundary condition in x-direction on the right.

Both tools are defined in a local coordinate system, annotated with " ' " in the left of Figure 3.3, which is the global Cartesian rotated by the tool angle α. The tool distance TD is defined in this local system, as the distance along its x-axis.

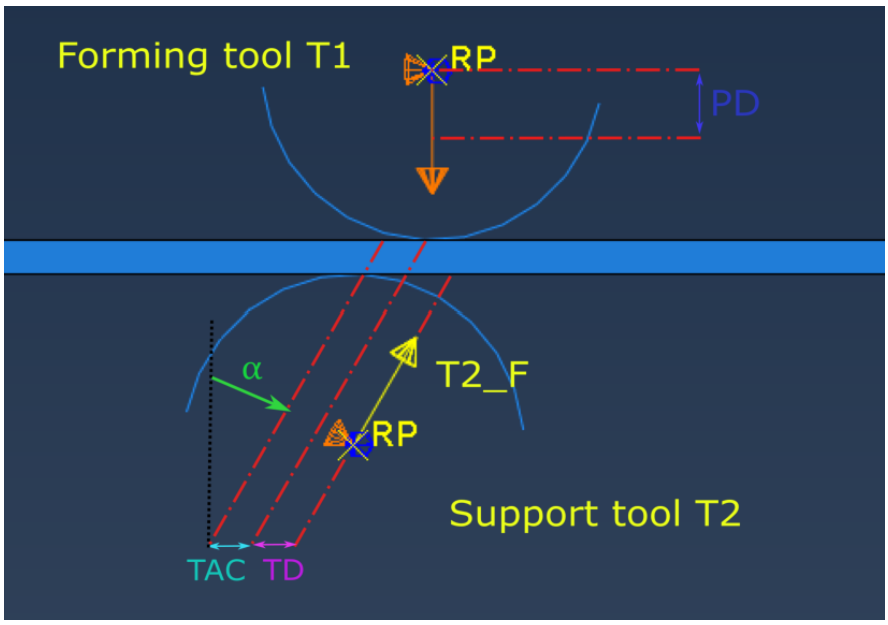

Figure 3.3: Detailed overview of simulation coordinate frames, loads and parameters. A local frame, frame $'$, is defined under tool angle α for the tool movement

3.1.5 Contact

Contact between the rigid tools and deformable sheet is modeled as a master-slave contact. The interaction property is modeled using normal behavior with ”hard” contact. No tangential phenomena are taken into account.

3.1.6 Model outputs

Field outputs are saved every last increment of each step. History outputs are generated for the reaction forces of the sheet clamps.

3.2 Simulation output analysis

A set of outputs need to be defined, in order to be able to define what a good product is, and to relate this to other process outputs such as process forces.

The field output PEEQ, which is plastic equivalent strain, is used to check that plastic deformation only occurs at the forming region between the tools. Although plastic deformation at the clamps may occur in some situations, it is desired to prevent plastic deformations outside the forming region. If successful, the zones outside of the forming region remain undeformed and thus flat.

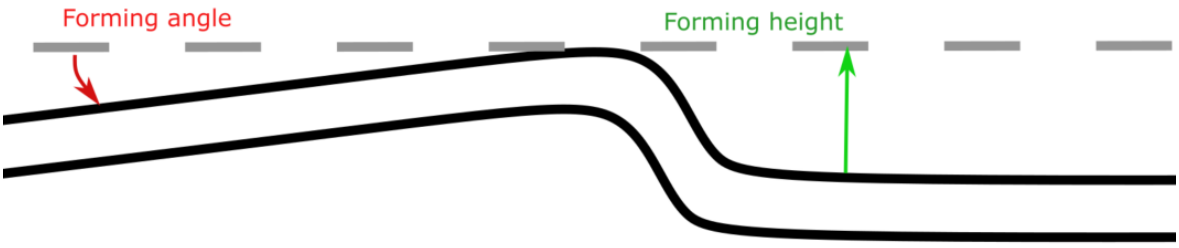

Figure 3.4: Demonstration of the output definitions forming height and forming angle.

The second field output to be evaluated is the set of nodal positions at the top of the sheet after each of the simulation stages (forming, tool release, clamp release). Due to the boundary conditions during clamp release, the model undergoes some rigid body rotation for some simulations. Therefore, the nodal positions are rotated in post-processing such that the right, undeformed part is horizontal. This is done by translating the right corner node to coordinate (0,0), calculating the angle of the right side by trigonometry and rotating it to zero, then translating the right corner node back to coordinate (100, 0).

This data can be used to assess the amount of springback after each stage and the geometrical accuracy of the final product with respect to the desired product shape. The forming angle is defined as the difference between the orientation of the left and right flat sections, outside of the forming region. The nodal positions are also used to calculate the forming depth and the forming angle. The forming depth is the difference in depth between the undeformed right side, and the maximum height close to the tool contact zone. This depth is divided by the pinch depth, to normalize the result. If the forming angle is positive, the maximum y-value of the rotated nodal values is taken. If the forming angle is negative, the maximum y-value in the neighborhood of the forming region is taken.

The reaction forces and moments of the clamped nodes are recorded as a history output. Sheet clamp reaction force and moment plots as a function of time can be generated. On the left edge, there can be forces in x- and y-direction. The forces in x-direction can cause a reaction moment, based on the nodal vertical distance to the middle of the sheet. On the right edge, no reaction forces in y-direction are possible, as the edge is free to move in that direction. Also here, a reaction moment is possible.

3.3 Simulations

Three different forming simulations will be used for parameter studies, each with their own goal. The goals are the following:

- The first goal is to see if it is possible to localize deformation using a support tool. A grid search with five parameters is used to get an initial idea of the possible results. The best performing results are selected on satisfaction based on certain criteria. For this (these) parameter set, a one-at-a-time parameter study is done in order to find the relation between forming results and the parameter input value.
- Then, a test is performed to characterize length gain of the strip based on the pinching force, pinching distance and the number of pinches.
- Finally, a full part is formed while trying to keep deformation local.

The python programming language is used to automate simulations and simulation outputs.

3.3.1 Single pinch to test locality

The 2D model described above along with its outputs is used for the first set of parameter variations where the tools deform the sheet once. The goal of this simulation is to proof if it is possible to localize plastic deformation, and maybe limit elastic deflection in other places during forming.

3.3.2 Sheet length strain characterization

Consider the 2D case, although it also works somewhat similar in 3D. To form a non-flat part from an originally flat shape, more material length is required. This needs to be generated out of the thickness direction, as plane strain is assumed. The desired length gain can be calculated geometrically when a part is designed. If one can relate this length gain to a support tool force, an initial prediction for support force based on desired length gain might be possible.
The model for this simulation is different in boundary conditions and tool control. The sheet is again clamped on the left, but free on the right. This allows the sheet to freely expand in length, thus finding the sheets desired elongation for a pinch with a certain force. Both tools are force controlled to the same force magnitude. Thus the sheet will remain in neutral, horizontal position. To find out if a future pinch will be influenced by previous pinches, a grid search is performed where the pinch distance

and pinch force is varied. The output will be the length gain per pinch of the sheet. If a combination of force and distance is found to be interacting with itself, the pinch distance will be varied in small steps for a constant force, in order to find a trend in the length gain behavior.

3.3.3 Multiple pinches to form a product

The idea of incremental sheet forming is to use multiple increments to form a part. Therefore, simulations with multiple pinches will be performed, in order to try to form a simple, undeep cup. The idea is that the effect of tool parameters will be more clear to see as it uses multiple pinches, and effects on a more realistic forming process might become clear.

The simulation works as follows. The tools move to a position close to where they should touch the sheet. The contact interaction between the tools and sheet is turned on. Then, in their local coordinate axis, they move towards the sheet. A virtual sensor is used based on contact force, which aborts the simulation when contact is made, and adjusts the boundary condition for the next step. Then, the next step is to pinch the sheet. After that, the contact interaction is turned off, and the tools are moved to the next position. This is repeated until the last pinch.

A virtual sensor and simulation restart are required, as for the second pinch and later, the sheet shape is not known before starting the simulation. Therefore, it is not known which part of the forming tool touches which part of the sheet first. Especially for the support tool this is important, as it switches from position to force control along one axis. Force control needs to have contact, otherwise it does not converge.

Chapter 4

Simulation results

4.1 Single pinch

For the single pinch, a parameter set was used for 5 variables:

Pinch depth	$=$	$[0.0, 0.1, 0.2, \ldots, 1.0]$	mm
Support force	$=$	$[20, 200, 400, 550, 700]$	N
Support tool angle	$=$	$[0.0, 15.0, 25.0, 35.0, 45.0]$	degrees
Tool distance	$=$	$[1.0, 1.75, 2.5, 3.25, 4.0, 4.75]$	mm
Tool force speed	$=$	$[0.5]$	seconds

Using tool forces above 700 Newtons often had convergence issues in the chosen simulation, which is why no higher forces are used. The tool force speed parameter has little influence on the output parameters, and is therefore not varied here.

A few moments during forming are shown in Figure 4.1. The first two plots are during the pinching step: the first is at 14% of the pinch movement, and then at the end of the pinch movement. The third and fourth are after tool contact release and after clamp release, respectively. The fourth image is what the final product will be. The stress increases gradually during pinching, due to movement of the upper tool and gradual increase of the forming force of the lower tool. After that, the stresses reduce. The remaining internal stresses are found by re-equilibrating the sheet after contact release. Note that the part has a rigid body rotation during the clamp release. This rotation is a simulation artifact. In later figures, where the nodal position is shown of the top side of the sheet, the nodes are rotated such that the right, flat part is horizontal and the symmetry condition at the right hand side of the model is maintained.

In Figure 4.2, six different forming results are shown with their PEEQ values. Their parameter values are shown in Table 4.1. Number 2 has undergone no plastic deformation, as the support tool force is too low to cause yielding. Both for small and high tool angle and pinch depth, plastic deformation is possible. The high pinch

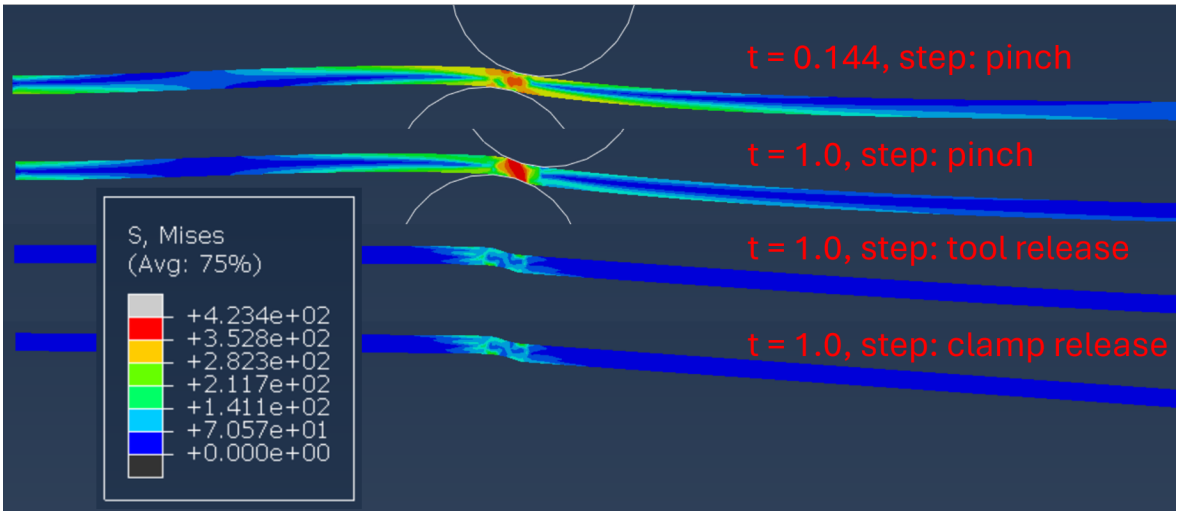

Figure 4.1: Von Mises stress during four forming steps. First two during pinching (time = 0.144 s, time = 1.0 s), then after tool release and after clamp release. Parameter values for the nominal case: tool angle 45 degrees, pinch depth 0.3 mm, tool distance 2.5 mm, tool force 550 N.

depth parameter set experiences some plastic deformation near the right clamp. This is caused by a high support tool force, which when combined with a reasonably high tool distance, it creates a moment that deforms the sheet before the forming tool moves down. This is not desirable. Between 1, 3 and 4, an increase in plastic deformation can be seen.

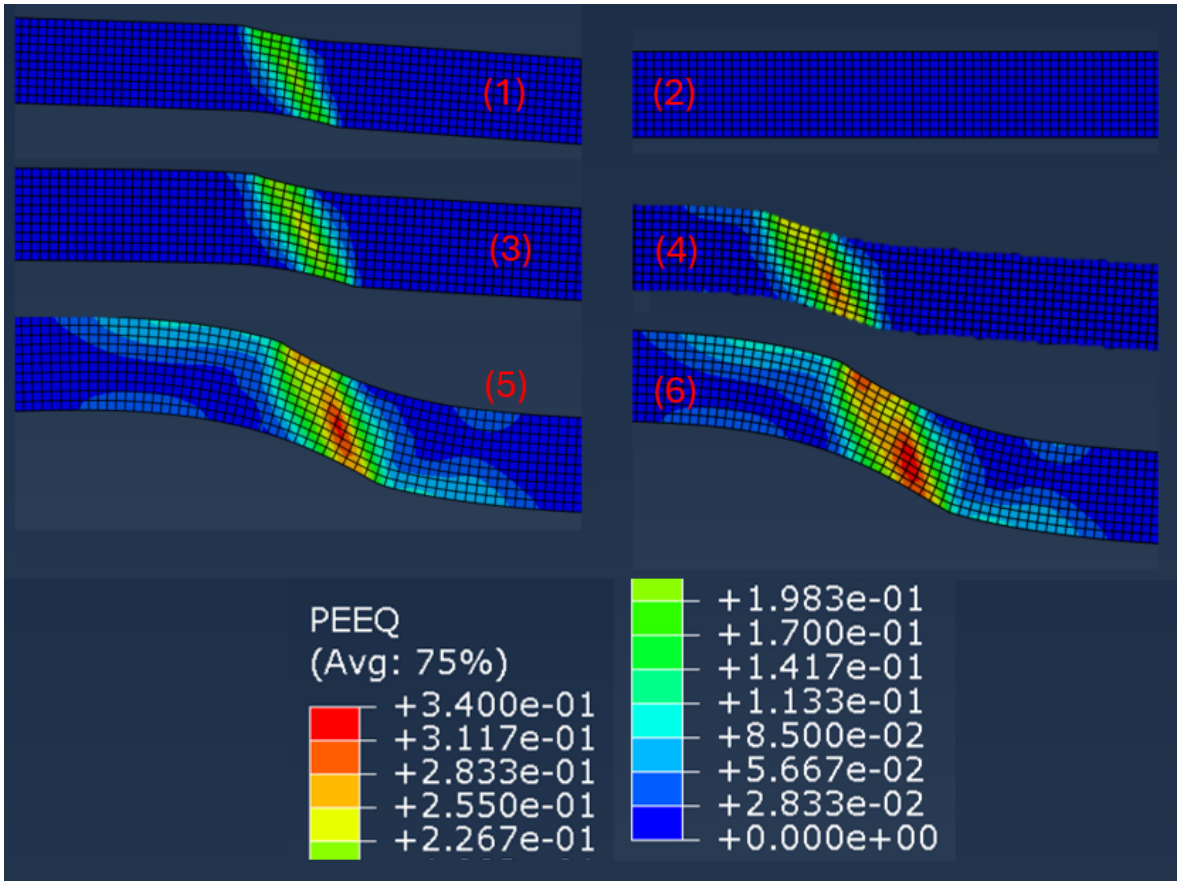

Figure 4.2: PEEQ field outputs for several parameter sets, all using the same color map. Their input and output parameters are given in Table 4.1

Table 4.1: Parameters used for the simulation study.

	TA	SD	TD	TF	TFS	FD	FA
1	0.00	0.1	1.75	550	0.5	1.14	2.25
2	0.00	1.0	1.75	20	0.5	0.00	0.00
3	0.00	0.5	2.50	550	0.5	0.33	3.09
4	45.0	0.3	2.50	550	0.5	1.02	3.75
5	45.0	0.5	4.75	550	0.5	1.72	4.83
6	45.0	1.0	4.75	550	0.5	1.02	2.69

The full simulation results can be evaluated based on the previously mentioned output criteria, namely forming depth and forming angle. Plotting these for all the parameter sets results in Figure 4.3. All data points are shown, and the color is related to one of the input parameters, namely tool angle. Quite some values have a high normalized forming height, where high means larger than one, as one is the target. This can be due to a high support force and large tool distance again, deforming the sheet more than the forming tool would when moving down. A small trend of zero

tool angle can be seen on the right bottom edge of the cloud of points. The cloud of points is also shown with colors for different input parameters, to perhaps find trends. For these, the figure axis is reduced, as a large region of the current figure is not interesting due to poor or unrealistic results.

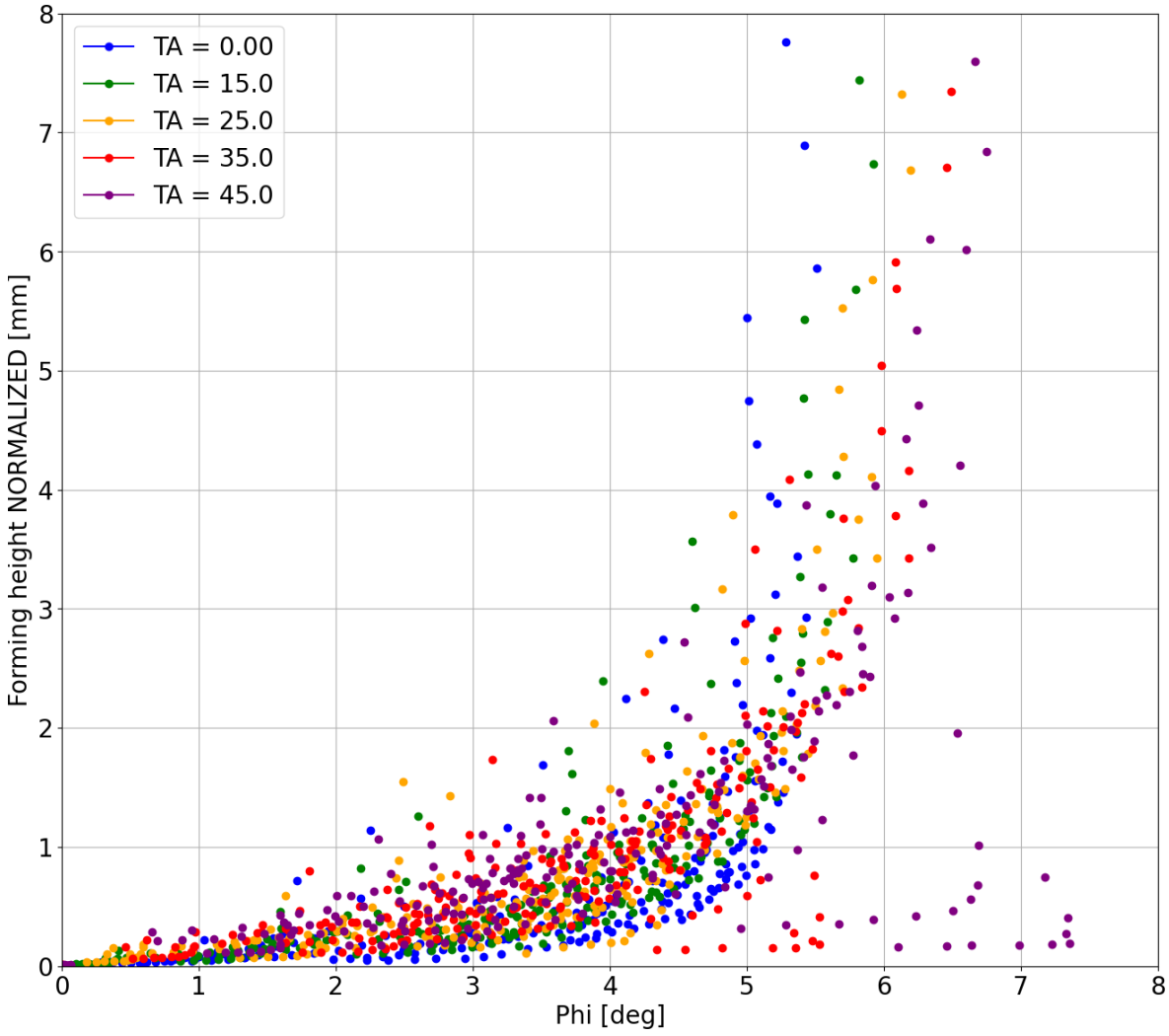

Figure 4.3: Grid search simulation, plotted in the selected output space of forming angle and forming height. Plot color depicts the tool angle.

Plotting the point cloud using colors to depict pinch depth results in Figure 4.4.

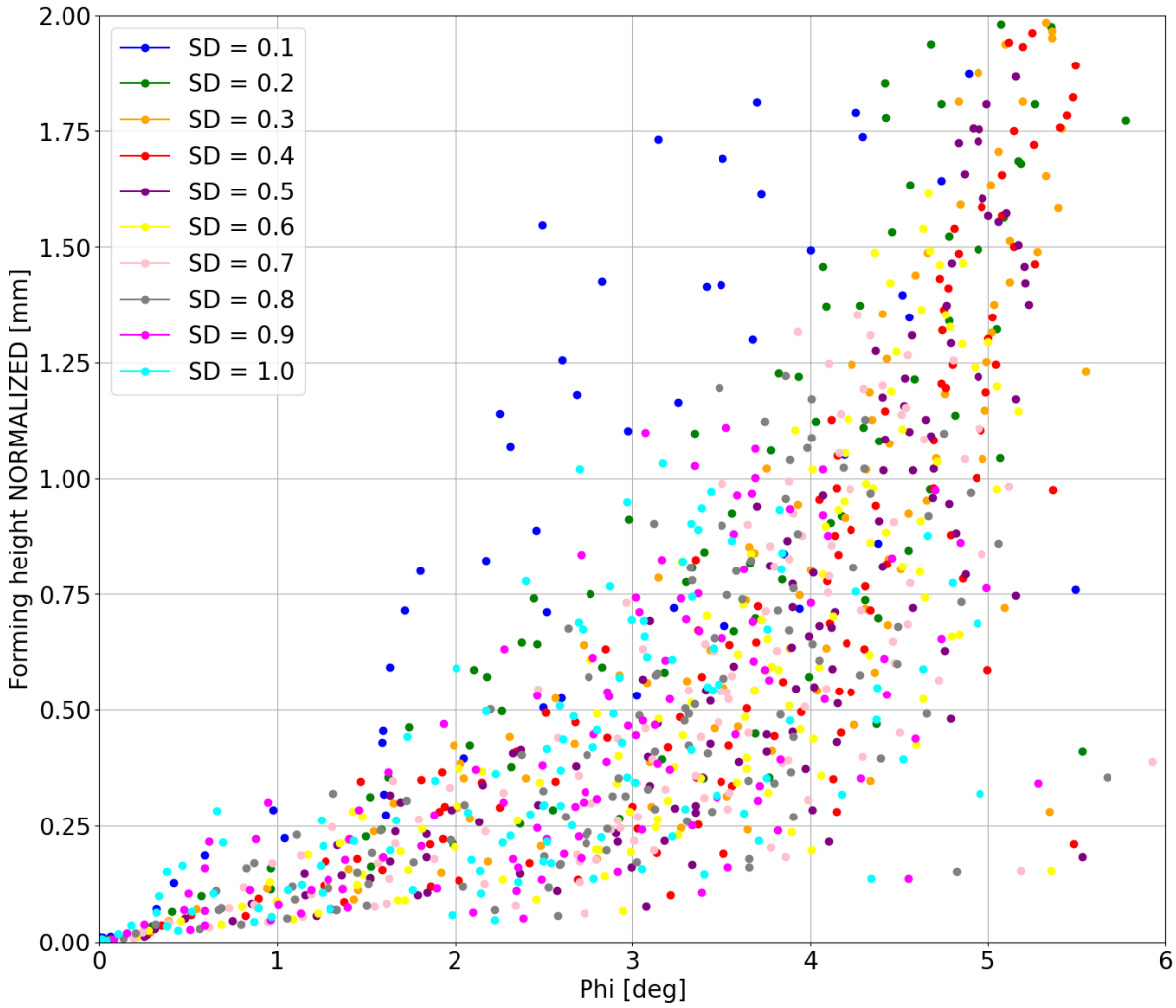

Figure 4.4: Grid search simulation, plotted in the selected output space of forming angle and forming height. Plot color depicts the pinch distance.

In general, one can see a trend of lower pinch depths resulting in higher normalized forming depths, and also a bit larger forming angles. The higher forming depths are more clustered together in the lower area.

The coloring can also be sorted in the increasing order for the other two input parameters. In Figure 4.5 it is sorted on tool distance, and in Figure 4.6 for tool force. For tool distance, the distances are more clustered together. From bottom left to top right, the clouds for higher tool distance start to appear. Around (0, 0) is an exception, as there mainly the results are shown for the lowest forming force. This is clearly shown in Figure 4.6, where all the lowest values are around this point. Higher forming forces are scattered around the plot.

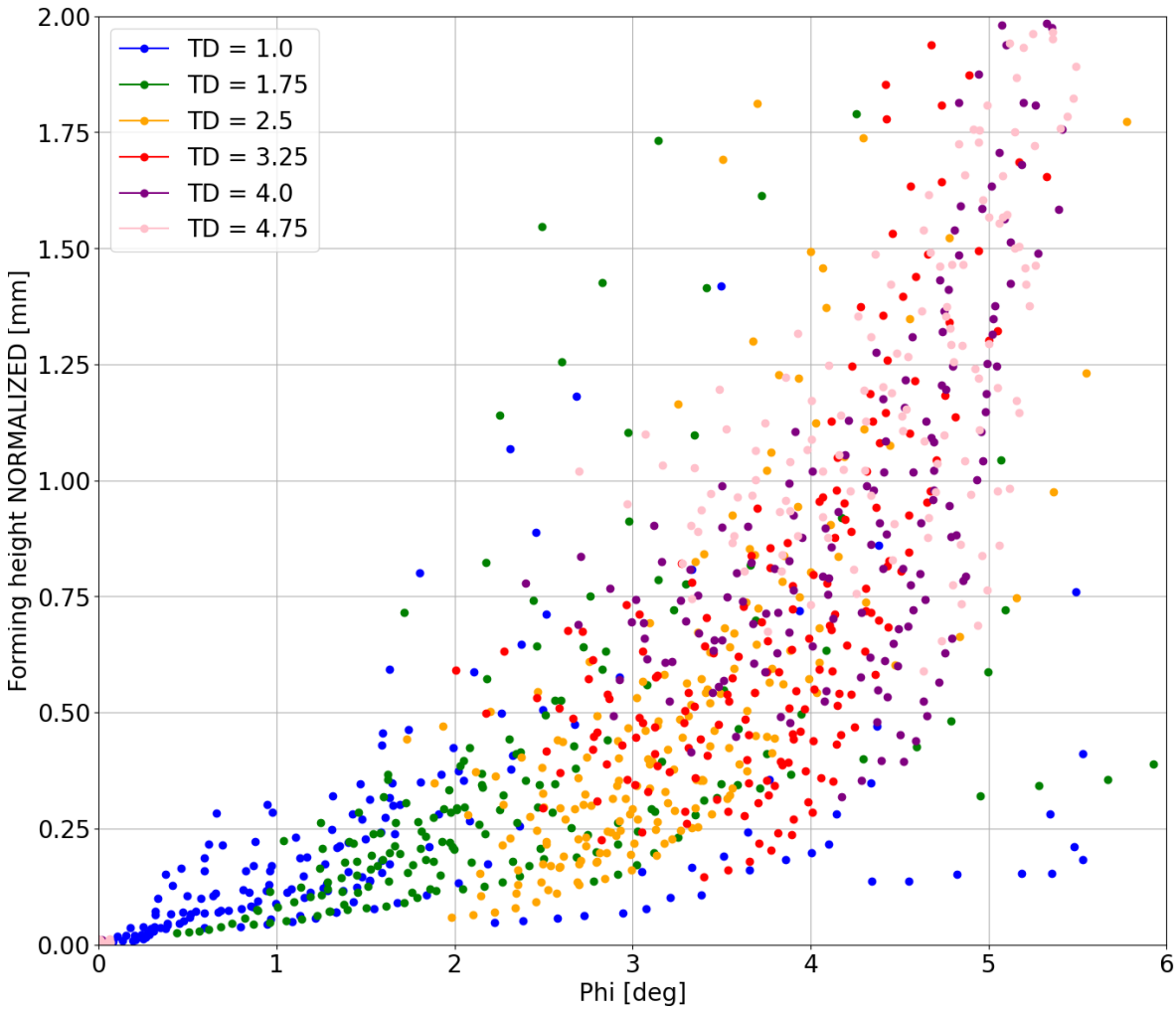

Figure 4.5: Grid search simulation, plotted in the selected output space of forming angle and forming height. Plot color depicts the tool distance.

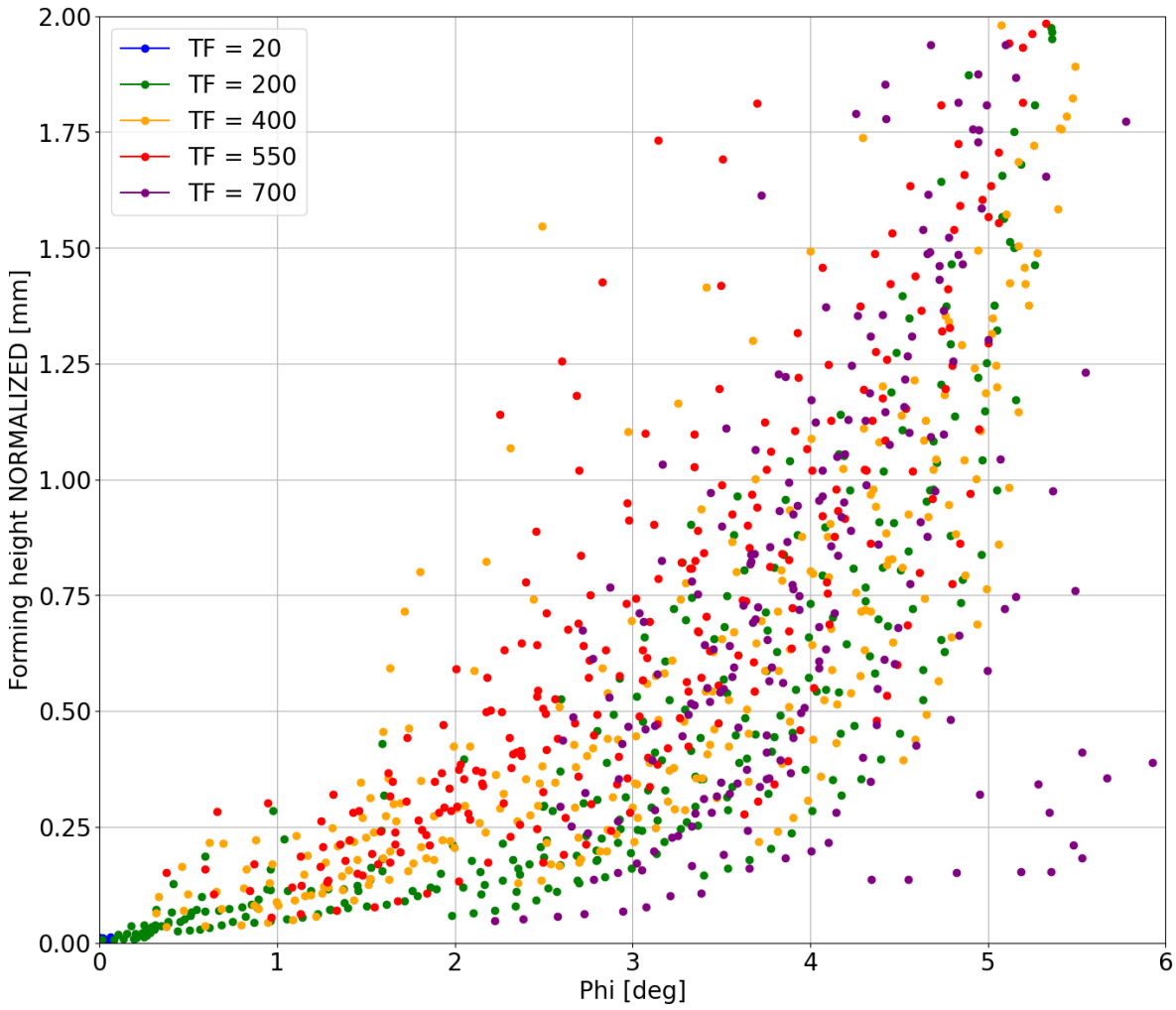

Figure 4.6: Grid search simulation, plotted in the selected output space of forming angle and forming height. Plot color depicts the support tool force.

4.1.1 Selected forming results

One parameter set can be selected as the nominal set. On this set, single parameters can be varied, to study their influence. The potential candidate sets for the single pinch are shown in Figure 4.7. For the forming depth, a 5% margin was selected to reduce the amount of options. Then, the lowest forming angle option is highlighted for every pinch depth, noted by the same color but a diamond marker. The high pinch depths are not chosen due to previously mentioned plastic deformation around the left clamp. Therefore, the parameter values for a pinch depth of 0.3 are chosen as preferable.

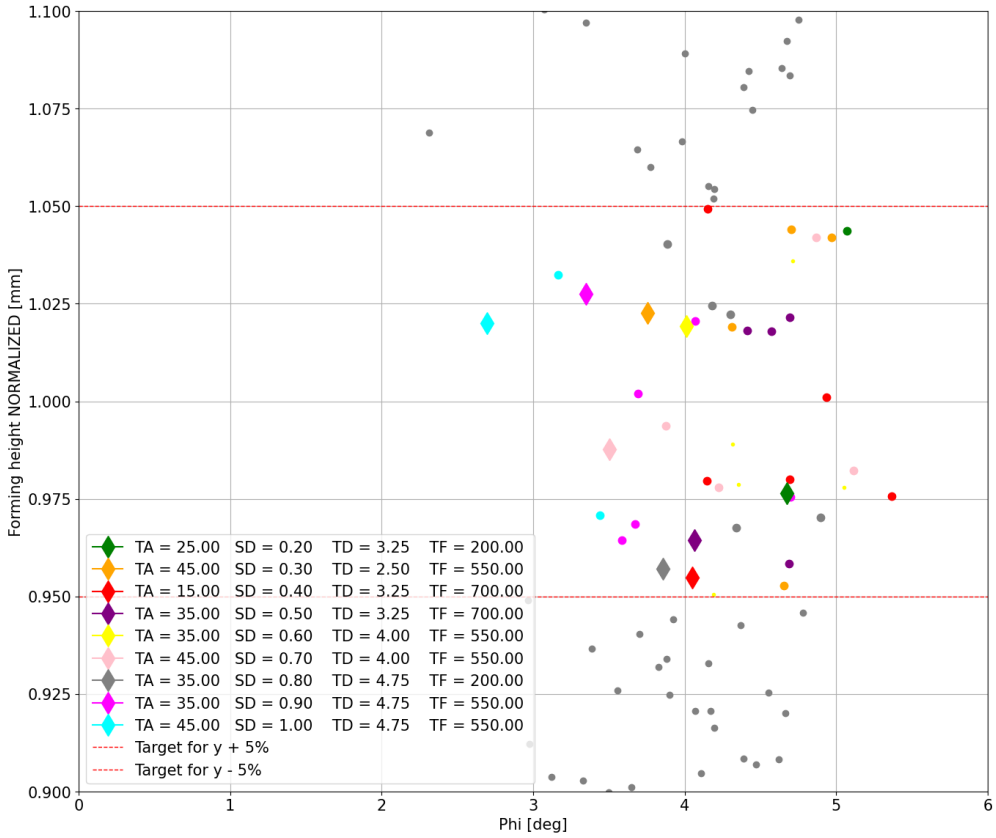

Figure 4.7: Output space of the grid run, with outputs selected for a normalized forming depth between 0.95 and 1.05.

The final nominal parameter set has input parameters of tool angle 45 degrees, pinch depth of 0.3 mm, with a tool distance of 2.5 mm at a force of 550N. This is used for single paramter variations in the next section.
For the multi-pinch simulation, the lowest forming angle in this band is chosen for

a tool angle of zero degrees. Currently, the multi-pinch simulation model does not incorporate tool angle yet.

4.1.2 Single parameter variation

Each input parameter is varied around its nominal value. The parameter values are:

Pinch depth	$=$	$[0.0, 0.1, 0.2, ..., 1.5]$	mm
Support tool force	$=$	$[25, 50, ..., 600, 610, ..., 700, 725, ...]$	N
Support tool angle	$=$	$[0.0, 2.5, ..., 72.5]$	degrees
Tool distances	$=$	$[1.0, 1.75, ..., 4.0]$	mm
Tool force speeds	$=$	$[0.5]$	seconds

The support tool force increments are reduced between 600 and 700 Newtons, to increase output space resolution. The effect of each input parameter on the outputs is demonstrated in Figre 4.8. Each input parameter can change the output values along a line. Some numerical outliers were removed, and simulations that did not fully converge are also taken out.

Almost all parameter changes result in a worse output, but this is expected, as the nominal case is chosen to be the best parameter combination that was included in the grid search. Tool force speed gives less change in outputs than the others. Quickly increasing tool force increases plastic deformation at low pinch depth, and in total increases the length gain more than a slower force increase. Very slow force means that the forming tool has moved down almost completely before the full force is exerted. The tool angle increases from zero to 72.5 degrees, where the forming depth increases gradually, and the forming angle reduces before it increases. This is similarly to the effect of tool distance. Pinch depth variation moves the output point along the edge of the cloud of points, as many pinch depths were included in the original grid search. With a very low tool force, no plastic deformation occurs, as mentioned earlier. At some point, it mainly increases forming depth. Then, the depth stays constant and the forming angle increases.

The relationship between each input and output parameter can be different for different nominal values, due to the high non-linearity of the forming process.

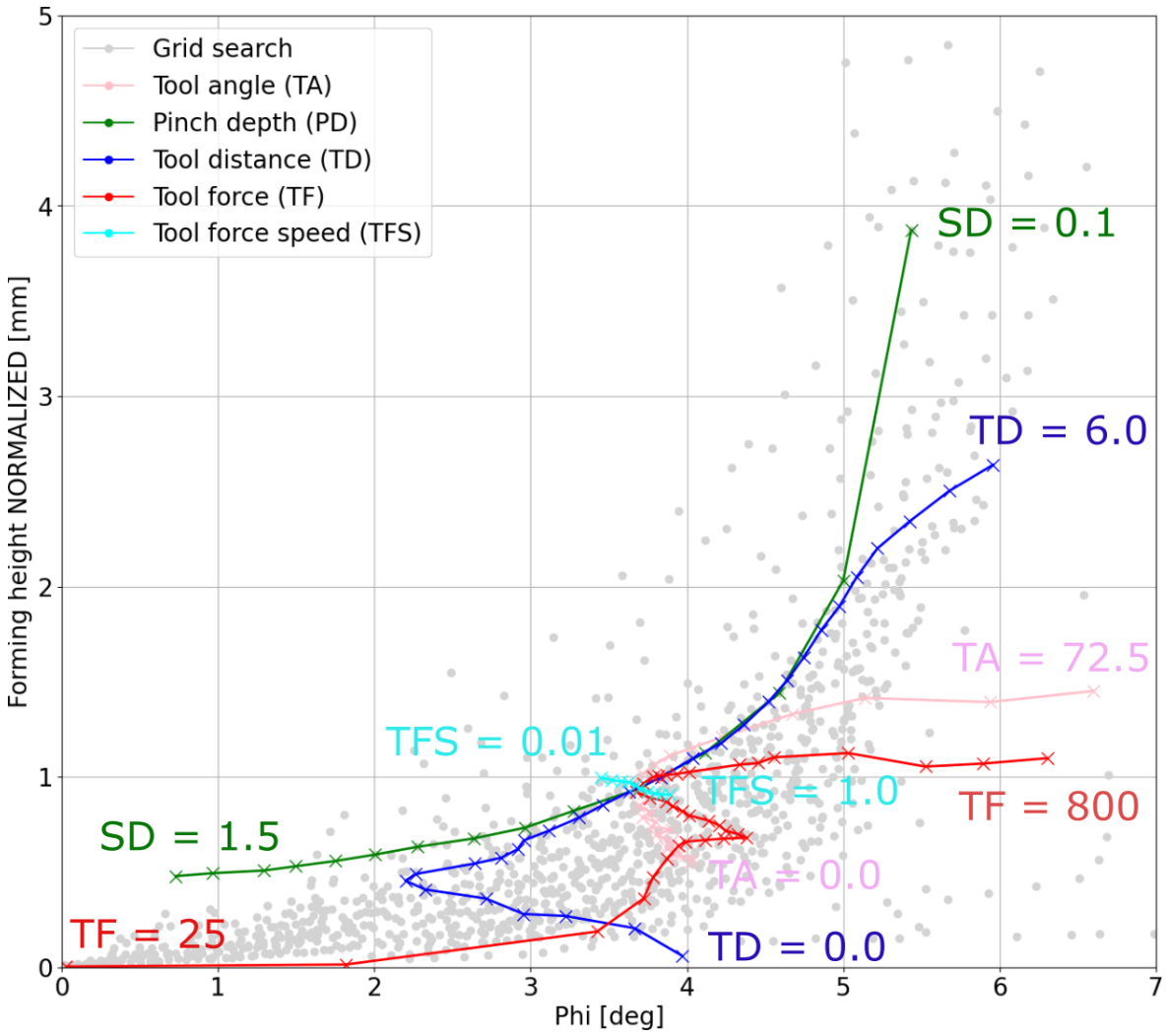

Figure 4.8: Single parameter variations of the nominal chosen parameter set, which is around coordinate (3.75, 0.95).

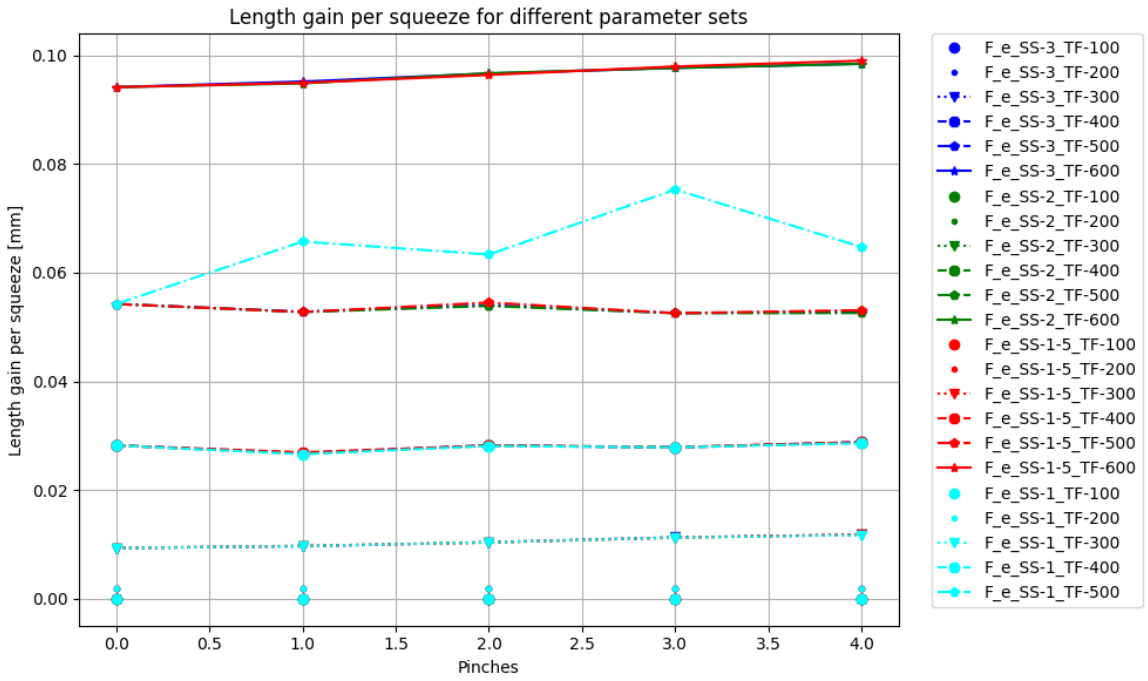

Figure 4.9: Length gain in mm per pinch, for different force values and larger pinch distances. In total 5 pinches. The value after SS indicates pinch distance, i.e. 3 means 3 mm shifts, and the forming force is the value after TF, so 100 to 600 Newtons.

4.2 Sheet length strain characterization

4.2.1 Varying pinch distances and forces

The length gain per pinch is used to compare the results. The parameter set is the following. The pinch distances are $\left[0.25,\ 0.50,\ 0.75,\ 1.0,\ 1.5,\ 2.0, 3\right]$, in mm, and the tool force values are $\left[100,\ 200,\ 300,\ 400,\ 500,\ 600\right]$ in Newtons. The results are shown in Figure 4.9 for pinch distances of 1 mm and larger, and in Figure 4.10 for 1 mm and smaller pinch distances.

For large pinch distances, almost all lines for a constant force overlap each other. This means that neighboring pinches do not influence each other. One line does not overlap, namely for a pinch distance of 1 mm and a tool force of 500 N. Decreasing the pinch distance results in pinches starting to influencing each other.

This parameter set is also plotted in a smaller pinch distance plot. For a constant force value, decreasing the pinch distance increases the neighboring influence. The previous deformation increases the stress in the material at the area of the next pinch. When it is pinched, it is easier to reach the yield stress and cause plastic deformation, causing thinning and thus length strain. For pinch distances of 0.5 mm

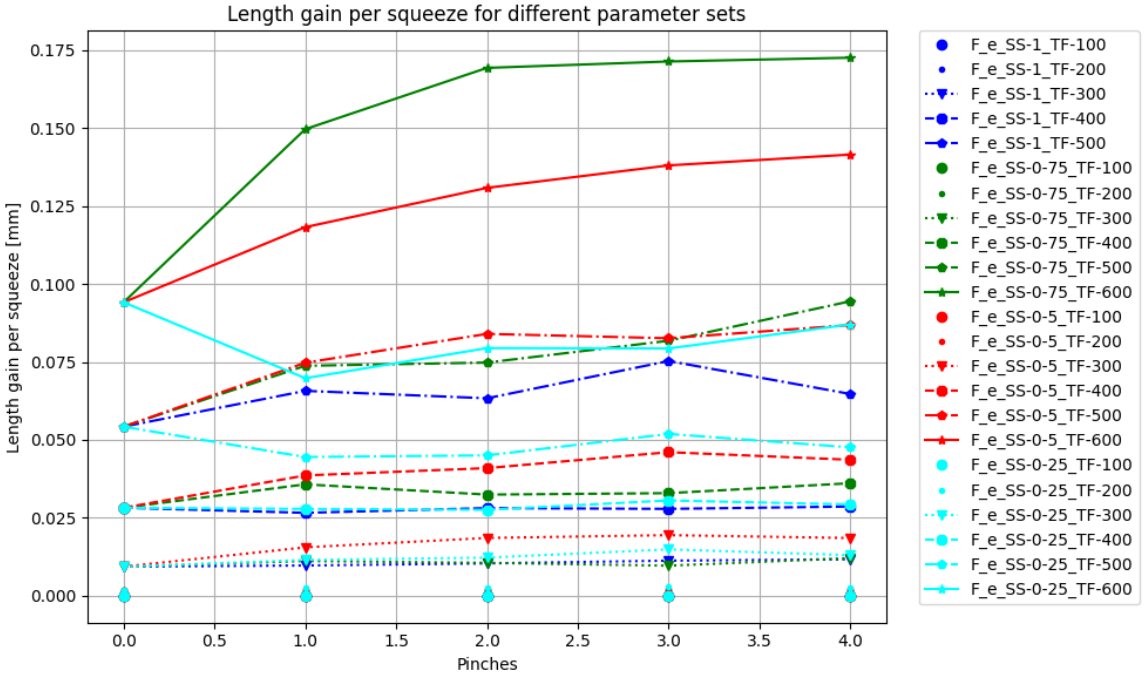

Figure 4.10: Length gain in mm per pinch, for different force values and smaller pinch distances. In total 5 pinches. The value after SS indicates pinch distance, i.e. 3 means 3 mm shifts, and the forming force is the value after TF, so 100 to 600 Newtons.

and larger, the pinch interaction increases the length gains. For a pinch distance of 0.25 mm at forces of 400 and higher, the pinch interaction decreases the length gains. The tools move too little to pinch on not-yet-fully deformed sheet material, for this specific set of parameters.

The simulation of 600 N for a pinch distance of 1 mm was not successfully finished, thus not plotted. For the three distances for 600 N, the larger the distance, the larger the length gain. It could be that previous pinches cause so much work hardening, that it is harder to deform at the next location. Also a convergence can be seen, which means that the stress at a fresh pinch point is at its maximum value possible, caused by work hardening of previous pinches.

4.2.2 Vary pinch distance for a set force

In the previous strain test, one could see that the length gain per pinch starts to increase when the pinch distance comes down to 1 mm, for a force of 500 N or larger. To further investigate this behavior, a second simulation is performed where the pinch distance is increased in smaller increments, for a force of 500 N. The pinch distances are $\left[0.1, 0.2, ..., 1.4, 1.5\right]$ mm. The sheet will be pinched ten times for each distance, and the results are shown in Figure 4.11.

For a pinch distance larger than 1 mm, one can see that the pinch strain remains constant, i.e. the current pinch is not affected by the work hardening of the previous pinch. The pinch distance is large enough, or the forming force is low enough.

From 1 mm onward, trends can be seen. For decreasing the distance down to around 0.7 mm, the pinch strain increases, and starts to converge after a few pinches. The pinches are influenced by previous work, but after enough pinches, the pinch strain becomes constant. The previous work hardening increases the stress in the material, thus reaching the yield stress with more ease.

Decreasing the distance further, decreases the pinch strain. For too small distances, the current piece of material being pinched, has undergone too much plastic deformation from the previous pinches. It has already been thinned, only a small part not yet, resulting in not much length gain.

To further investigate above trend, the Von Mises stress and PEEQ are plotted. In Figure 4.12, the Von Mises stress states are shown at the end of the first, fifth and tenth pinch. The maximum stress increases gradually, indicated by a larger dark red spot. The work hardening influences future pinches. Also in the plastic strain plots of Figure 4.13, work hardening effect can be seen. The bottom sheet has a pinch distance of 1.2 mm, which is large enough for the current force, to not have influence of previous deformations. Decreasing the pinch distance to 0.6 mm shows that the amount of work hardening is increasing every pinch. Finally, in the top figure, the

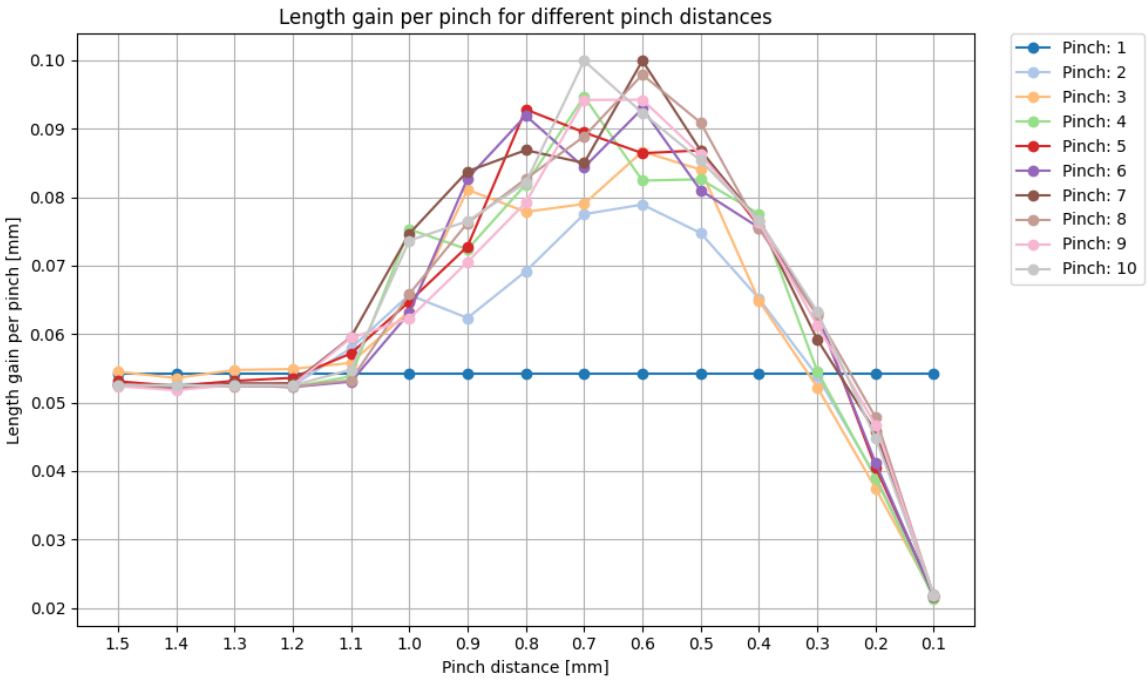

Figure 4.11: Length increase of the sheet with a free edge on the right, for several pinch distances with a constant tool force of 500 N

pinch distance of 0.2 mm is small enough that there is too much work hardening for the amount of tool movement.

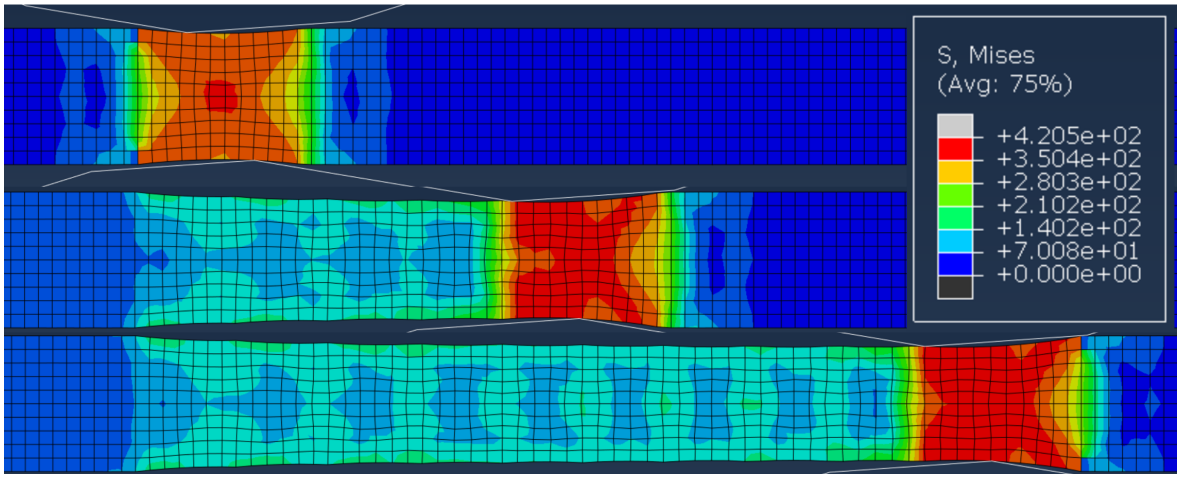

Figure 4.12: Von Mises stresses at the end of the first, fifth and tenth pinch, with a pinch distance of 0.6 mm

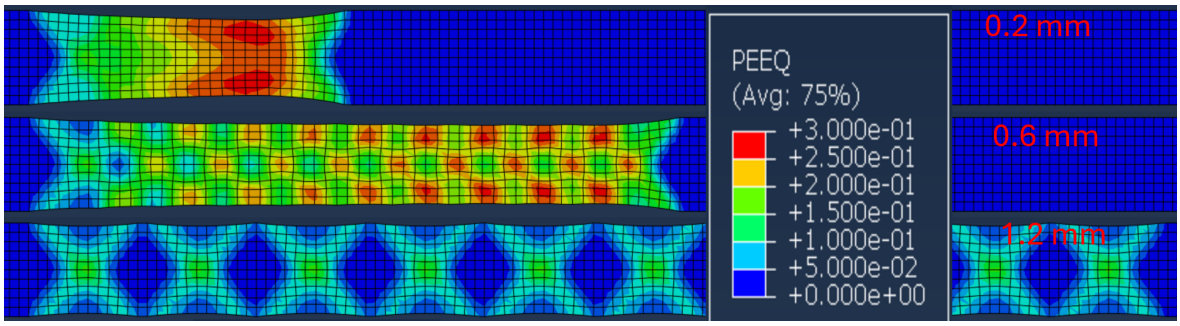

Figure 4.13: PEEQ field outputs on fixed scale, for 500 N and three pinch distances

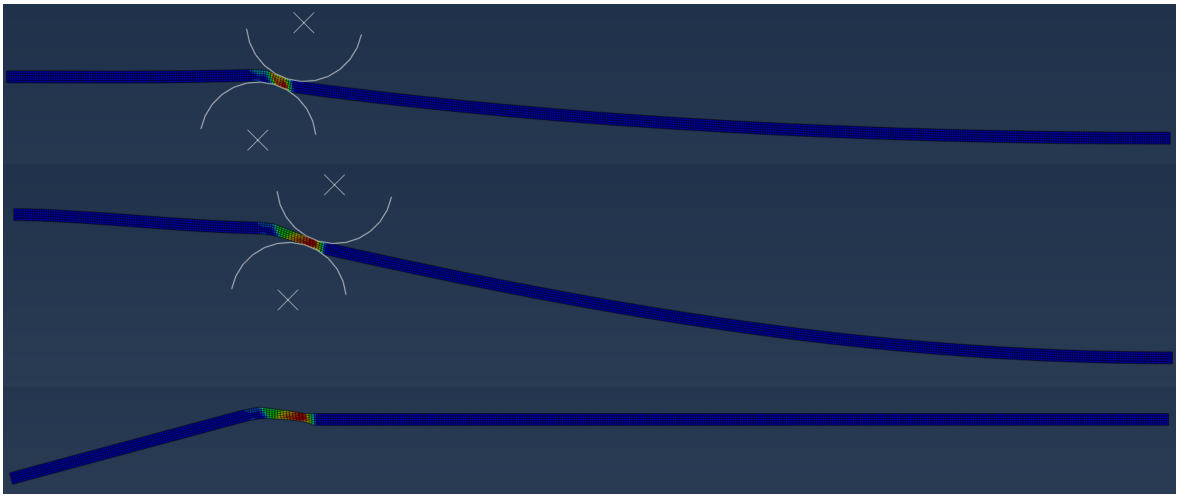

Figure 4.14: PEEQ of the multi-pinch forming for zero tool angle. First two pictures are at the end of the third and of the tenth pinch, respectively. The last picture is after the clamps have been removed. The darkest red indicates a large strain of 50%.

4.3 Multiple pinches

Using the mentioned parameter set of zero tool angle with a pinch depth of 0.5 mm, tool distance of 4.0 mm, support force of 550 N, 10 pinches are performed with a horizontal distance between pinches of also 0.5 mm. The forming process is shown in Figure 4.14. The final forming depth is 0.5 mm, in the situation after clamp release. The final forming angle is 15 degrees. The results do not correspond with the single pinch parameter results. After the first pinch, the sheet shape is different, therefore, other parameters might be more appropriate. Also, some little plastic deformation has occurred around the left clamp.

Chapter 5

Discussion, conclusions and recommendations

5.1 Discussion

A clear influence of the chosen support tool parameters on the forming results can be seen, indicating that improving forming with a support tool is possible with appropriate parameters. The input parameters are treated individually. However, due to the definition of tool distance, tool distance has some relation to tool angle, which could skew results. Also, normalized forming depth is used as one of the two output parameters. Using a low depth but a high tool distance and force can still result in significant plastic deformation and forming height. Normalizing this height using the input depth can give results up to a value of eight, which is inappropriate.

This research was conducted based on 2D simulations. The simulations did not incorporate effects such as friction, with unknown influence on the forming results. The forming in 2D is significantly different from the 3D case, which should not be forgotten.

5.2 Conclusion

5.2.1 Single pinch

It can be concluded that deforming the sheet plastically around the tool tips is possible with some satisfaction for a support force of 200 N or higher, where the other parameters can have various values. For large tool distances and pinch depths, deformations do not remain local, due to the forming force causing plastic strain by bending.

5.2.2 Length strain characterization

There are clear effects visible between forming force and distance between pinches. For a given forming force, the forming distance can be increased such that the pinches do not influence each other. For forming, this is undesirable, as the step increments would remain very large and less detailed forming is possible. There are forming distances, where the interaction effects increase until a limit is reached.

5.2.3 Multiple pinches

The results from a single pinch do not directly translate to the multiple pinches simulation. No pinch interaction was taken into account in determining the parameters used. Also, the deformed sheet has a different shape, thus other parameters could be more appropriate.

5.3 Recommendations

In the future, for this research, it can be interesting to look at relations between input parameters, to find out when the other input values are appropriate for one chosen parameter. More simulations for multiple pinches can be performed, to study the accumulation of the effects of input and output parameters where the difference in results might be more noticeable. Perhaps a parameter search could be performed based on these simulations, or the forming parameters could be optimized for every individual pinch for a specific product. Also, the 2D case seems sufficiently different from 3D. Analyze in 3D wether or not results in 2D correspond in some way to the real world process. Otherwise, 2D experiments could be performed for incremental strip forming, to check correspondence with the 2D simulation model.

Bibliography

[1] J. M. Allwood, G. P. F. King, and J. Duflou, “A structured search for applications of the incremental sheet-forming process by product segmentation,” *Proceedings of the Institution of Mechanical Engineers, Part B: Journal of Engineering Manufacture*, vol. 219, no. 2, pp. 239–244, Feb. 2005. [Online]. Available: https://journals.sagepub.com/doi/10.1243/095440505X8145

[2] Taiwan SCN, “Car body panel press 2000ton for automotive industry,” https://www.youtube.com/watch?v=RgcGtlJ6R1w, [Online; accessed 01-January-2025].

[3] J. R. Duflou, A.-M. Habraken, J. Cao, R. Malhotra, M. Bambach, D. Adams, H. Vanhove, A. Mohammadi, and J. Jeswiet, “Single point incremental forming: state-of-the-art and prospects,” *International Journal of Material Forming*, vol. 11, no. 6, pp. 743–773, Nov. 2018. [Online]. Available: http://link.springer.com/10.1007/s12289-017-1387-y

[4] H. Y. Shahare, A. K. Dubey, P. Kumar, H. Yu, A. Pesin, D. Pustovoytov, and P. Tandon, “A Comparative Investigation of Conventional and Hammering-Assisted Incremental Sheet Forming Processes for AA1050 H14 Sheets,” *Metals*, vol. 11, no. 11, p. 1862, Nov. 2021. [Online]. Available: https://www.mdpi.com/2075-4701/11/11/1862

[5] Ammar Kalo, “Spif setup,” https://www.ammarkalo.com/Incremental-Sheet-Metal-Forming, online; accessed 01-January-2025.

[6] H. Lu, “Investigation of control of the incremental forming processes,” PhD Thesis, The University of Queensland, Jun. 2017. [Online]. Available: http://espace.library.uq.edu.au/view/UQ:612878

[7] N. Moser, “Deformation mechanisms and process planning in double-sided incremental forming,” Dec. 2019. [Online]. Available: https://www.researchgate.net/publication/336812662_Deformation_Mechanisms_and_Process_Planning_in_Double-Sided_Incremental_Forming

[8] Amino North America Corporation, “Nc dieless forming (rapid prototyping),” https://www.aminonac.ca/nc-dieless-forming-rapid-prototyping/, [Online; accessed 01-January-2025].

[9] M. Amino, M. Mizoguchi, Y. Terauchi, and T. Maki, “Current Status of “Dieless” Amino’s Incremental Forming,” *Procedia Engineering*, vol. 81, pp. 54–62, 2014. [Online]. Available: https://linkinghub.elsevier.com/retrieve/pii/S1877705814012296

[10] SmarterEveryday, “Roboforming: Behind the scenes as machina labs (the future of metalworking) - smarter every day 290b,” www.youtube.com/watch?v=Jc16Ob-yoDs, 2023, [Online; accessed 01-January-2025].

[11] Machina Labs, “Design guide of idf parts,” https://machinalabs.ai/resources/machina-labs-design-guidelines, [Online; accessed 01-January-2025].

[12] H. Ren, J. Xie, S. Liao, D. Leem, K. Ehmann, and J. Cao, “In-situ springback compensation in incremental sheet forming,” *CIRP Annals*, vol. 68, no. 1, pp. 317–320, 2019. [Online]. Available: https://linkinghub.elsevier.com/retrieve/pii/S000785061930068X

[13] K. Maji and G. Kumar, “Inverse analysis and multi-objective optimization of single-point incremental forming of AA5083 aluminum alloy sheet,” *Soft Computing*, vol. 24, no. 6, pp. 4505–4521, Mar. 2020. [Online]. Available: http://link.springer.com/10.1007/s00500-019-04211-z

[14] M. Crenganiș, A. Bârsan, S.-G. Racz, and M. D. Iordache, “Single point incremental forming using kuka kr6-2 industrial robot - a dynamic approach,” https://www.researchgate.net/publication/329801281_SINGLE_POINT_INCREMENTAL_FORMING_USING_KUKA_KR6-2_INDUSTRIAL_ROBOT-A_DYNAMIC_APPROACH, 2018, .

[15] H. Mostafanezhad, H. G. Menghari, S. Esmaeili, and E. M. Shirkharkolaee, “Optimization of two-point incremental forming process of AA1050 through response surface methodology,” *Measurement*, vol. 127, pp. 21–28, Oct. 2018. [Online]. Available: https://linkinghub.elsevier.com/retrieve/pii/S026322411830318X

[16] Northwestern University, “titel opzoeken - bron zoeken, welke? nw site? nw paper beter miss,” https://ampl.mech.northwestern.edu/research/current-research/incremental-forming-machines.html, [Online; accessed 01-January-2025].

[17] Trajectory Ventures, “Machina labs unveils portable ai robotics system for metal forming for
agile manufacturing at fabtech,” [Online; accessed 01-January-2025]. [Online]. Available: https://trajectoryventures.vc/investments-news/machina-labs-unveils-portable-ai-robotics-system-for-metal-forming-for-agile-manufacturir

[18] K. Jackson and J. Allwood, “The mechanics of incremental sheet forming,” *Journal of Materials Processing Technology*, vol. 209, no. 3, pp. 1158–1174, Feb. 2009. [Online]. Available: https://linkinghub.elsevier.com/retrieve/pii/S0924013608002422

[19] O. Music and J. M. Allwood, “The use of spatial impulse responses to characterise flexible forming processes with mobile tools,” *Journal of Materials Processing Technology*, vol. 212, no. 5, pp. 1139–1156, May 2012. [Online]. Available: https://linkinghub.elsevier.com/retrieve/pii/S0924013612000040

[20] H. Ren, F. Li, N. Moser, D. Leem, T. Li, K. Ehmann, and J. Cao, “General contact force control algorithm in double-sided incremental forming,” *CIRP Annals*, vol. 67, no. 1, pp. 381–384, 2018. [Online]. Available: https://linkinghub.elsevier.com/retrieve/pii/S0007850618300817

[21] Z. Chang, M. Yang, and J. Chen, “Geometric deviation during incremental sheet forming process: Analytical modeling and experiment,” *International Journal of Machine Tools and Manufacture*, vol. 198, p. 104160, May 2024. [Online]. Available: https://linkinghub.elsevier.com/retrieve/pii/S0890695524000464

[22] N. Moser, J. Cao, and K. Ehmann, “Ampl toolpaths – user guide,” https://ampl.mech.northwestern.edu/research/current-research/ampltoolpaths.html, [Online; accessed 01-January-2025].

[23] R. Malhotra, J. Cao, F. Ren, V. Kiridena, Z. Cedric Xia, and N. V. Reddy, “Improvement of Geometric Accuracy in Incremental Forming by Using a Squeezing Toolpath Strategy With Two Forming Tools,” *Journal of Manufacturing Science and Engineering*, vol. 133, no. 6, p. 061019, Dec. 2011. [Online]. Available: https://asmedigitalcollection.asme.org/manufacturingscience/article/doi/10.1115/1.4005179/439927/Improvement-of-Geometric-Accuracy-in-Incremental

[24] N. Bari and S. Kumar, “Multi-stage single-point incremental forming: an experimental investigation of thinning and peak forming force,” *Journal of the Brazilian Society of Mechanical Sciences and Engineering*, vol. 45, no. 3, p. 137, Mar. 2023. [Online]. Available: https://link.springer.com/10.1007/s40430-023-04055-7

[25] S. Tanaka, “Incremental sheet metal formed square-cup obtained through multi-stepped process,” *Procedia Manufacturing*, vol. 15, pp. 1170–1176, 2018. [Online]. Available: https://linkinghub.elsevier.com/retrieve/pii/S2351978918310680

[26] F. Han, J.-h. Mo, P. Gong, and M. Li, “Method of closed loop springback compensation for incremental sheet forming process,” *Journal of Central South University*, vol. 18, no. 5, pp. 1509–1517, Oct. 2011. [Online]. Available: http://link.springer.com/10.1007/s11771-011-0867-3

[27] O. Music and J. M. Allwood, “The use of spatial impulse responses to characterise flexible forming processes with mobile tools,” *Journal of Materials Processing Technology*, vol. 212, no. 5, pp. 1139–1156, May 2012. [Online]. Available: https://linkinghub.elsevier.com/retrieve/pii/S0924013612000040

[28] C. Wang, A. He, S. Liu, and P. A. Meehan, “Learning-based model predictive control for two-point incremental sheet forming,” *Journal of Manufacturing Processes*, vol. 105, pp. 187–198, Nov. 2023. [Online]. Available: https://linkinghub.elsevier.com/retrieve/pii/S1526612523008939